

Partitioning the phenotypic variance of reaction norms

Pierre de Villemereuil^{1,2} and Luis-Miguel Chevin³

¹*Institut de Systématique, Évolution, Biodiversité (ISYEB), École Pratique des Hautes Études PSL, MNHN, CNRS, SU, UA, Paris, France*

²*Institut Universitaire de France (IUF)*

³*CEFE, CNRS, Université de Montpellier, Université Paul Valéry Montpellier 3, EPHE, IRD, Montpellier, France*

Keywords: phenotypic plasticity, quantitative genetics, character-state approach, polynomial approach, non-linear modelling

Corresponding author: Pierre de Villemereuil, E-mail: pierre.de-villemereuil@mnhn.fr

Abstract

Many phenotypic traits vary in a predictable way across environments, as captured by their norms of reaction. These reaction norms may be discrete or continuous, and can substantially vary in shape across organisms and traits, making it difficult to compare amounts and types of plasticity among (and sometimes even within) studies. In addition, the evolutionary potential of phenotypic traits in heterogeneous environments critically depends on how reaction norms vary genetically, but there is no consensus on how this should be quantified. Here, we propose a partitioning of phenotypic variance across genotypes and environments that jointly address these challenges. We start by distinguishing the components of phenotypic variance arising from the average reaction norm across genotypes, (additive) genetic variation in reaction norms, and a residual that cannot be predicted from the genotype and the environment. We then further partition the (additive) genetic variance of the trait into a component related the marginal (additive) genetic variance in the trait and a component due to (additive) genetic variance in plasticity, including for complex, non-linear reaction norms. The last step involves estimating contributions from different parameters of reaction norm shape to these variance components. This decomposition is general and we show how to apply it to various modelling approaches, from the character-state to curve-parameter approaches, including polynomial functions, or arbitrary non-linear models. To facilitate the use of this variance decomposition, we provide the Reacnorm R package, including a practical tutorial. Overall the toolbox we develop should serve as a base for an unifying and deeper understanding of the variation and genetics of reaction norms and plasticity, as well as more robust comparative studies of plasticity across organisms and traits.

22 Introduction

23 The phenotype of a given genotype can vary in response to its environment of development or expres-
24 sion, through a phenomenon broadly described as phenotypic plasticity (Schlichting & Pigliucci 1998;
25 Bradshaw 1965). Phenotypic plasticity is currently attracting considerable interest in the context of
26 rapidly changing natural environments (Gienapp et al. 2008; Chevin et al. 2010; Merilä & Hendry
27 2014). While the mere existence (and even prevalence) of phenotypic plasticity is uncontroversial, its
28 relative contribution to observed or predicted phenotypic change in the wild (Teplitsky et al. 2008;
29 Gienapp et al. 2008; Merilä & Hendry 2014; Bonamour et al. 2019), as well as the extent of its inter-
30 play with population-level processes such as natural selection and population dynamics (Reed et al.
31 2010; Vedder et al. 2013; Schaum & Collins 2014; de Villemereuil et al. 2020), are very active research
32 areas. Answering these questions requires for biologists to be able to dissect and compare phenotypic
33 plasticity in detail in a wide range of traits, environmental contexts and species. This requires a
34 methodology that is appropriate for each context, while being general enough to be comparable across
35 context.

36 The relationship between the phenotype and the environment is captured by the reaction norm (or
37 norm of reaction), which is defined at the level of genotypes (Woltereck 1909; Schlichting & Pigliucci
38 1998). Reaction norms encompass phenotypic responses to both continuous environments (such as
39 temperature, salinity, etc.) and categorical/discrete ones (such as host plant for a phytophagous
40 insect). Within a simple model of reaction norm, quantifying plasticity may be straightforward. For
41 instance, both empirical (Charmantier et al. 2008; Nussey et al. 2005) and theoretical (Gavrilets &
42 Scheiner 1993b; Lande 2009) work have extensively relied on the assumption of a linear reaction
43 norm, whose slope is used as a metric of plasticity, since it quantifies how much phenotypic change is
44 induced per unit environmental change. However, regression slopes are signed and have units of trait
45 per environment, so even in this simple case some standardization is needed in order to compare the
46 magnitude of plasticity among studies. Beyond this simple scenario, drawing robust conclusions about
47 phenotypic plasticity requires being able to quantify and compare its magnitude across organisms,
48 traits and environments, in a way that is applicable across the statistical frameworks used to study
49 plasticity.

50 Beyond *how much* phenotypes change with the environment, *how* they change can also be of
51 importance. First, different reaction norm shapes may come with different biological interpretations.
52 For instance, a bell-shaped (eg quadratic, Gaussian) reaction norm may indicate that some mechanism
53 underlying a measured trait is maximized at an intermediate value of the environment. This is often

54 expected for traits that are direct components of fitness, or that can be interpreted as proxies for
55 performance, for which the reaction norms are generally termed tolerance or performance curves
56 (Lynch & Gabriel 1987; Deutsch et al. 2008; Angilletta 2009). A sigmoid shape, on the other hand,
57 may indicate that plasticity is directional but that the range of possible phenotypes is constrained, or
58 that selection favors discrete-like variation (Moczek & Emlen 1999; Suzuki & Nijhout 2006; Hammill et
59 al. 2008; Chevin et al. 2013). Second, most theoretical models on the evolution of plasticity, especially
60 those based on quantitative genetics which are most directly comparable to empirical data, assume
61 a given reaction norm shape - often linear for simplicity (Scheiner 1993b; Tufto 2000; Lande 2009).
62 The extent to which theoretical predictions on the evolution of plasticity apply to any particular
63 empirical system thus depends on how well the reaction norm shape assumed in the models conforms
64 to observations in this system. In other words, we need some metric for whether a reaction norm
65 is "mostly linear" or "mostly curved", for instance. In addition, when fitting a particular model of
66 reaction norm shape to an empirical dataset, we would like to know how well this model captures the
67 overall plastic variation of the trait across environments.

68 A third crucial question regarding reaction norms is how (and how much) they vary genetically.
69 It has long been recognized that plasticity can evolve if reaction norms vary genetically (Bradshaw
70 1965), and theory has predicted how different aspects of reaction norm shape are expected to respond
71 to selection in a variable environment (de Jong 1990; Gomulkiewicz & Kirkpatrick 1992; Gavrillets &
72 Scheiner 1993b). However this theory has been little applied empirically, except for predictions about
73 the slope of linear reaction norms (or phenotypic differences between two environments). But beyond
74 this, it should also be of interest to identify which aspects of reaction norm shape are more likely
75 to evolve, based on how they vary genetically. For instance, a reaction norm may be highly curved
76 (e.g. quadratic) but have little genetic variability in curvature, instead mostly varying in position,
77 height, or local slope. Distinguishing between the genetic variance of the trait, marginalised across
78 environments, and the genetic variance of plasticity itself, can also be a conceptual and methodological
79 challenge. There is thus a need to compare genetic variation in different components of reaction norm,
80 but previous attempts to do so (in a meta-analysis) were limited by methodological obstacles (Murren
81 et al. 2014, see [Appendix G](#)). In fact, comparing genetic variation in the slope versus curvature of a
82 reaction norm, for instance, is not straightforward, as these parameters have different scales and even
83 units (trait per environment, vs trait per squared environment). More, even the notion of average slope
84 and curvature can have different meanings depending on the assumed distribution for the environment.
85 Genetic variation in reaction reaction norm shape can be analyzed by estimating variation in the
86 parameters of a continuous function of the environment, as done by the flexible framework of function-

87 valued traits (Kirkpatrick & Heckman 1989; Gomulkiewicz & Kirkpatrick 1992; Stinchcombe et al.
88 2012). In addition, it would be useful to be able to compare the relative contributions of variation in
89 different aspects of reaction norm shape to the overall variance in plasticity of a trait.

90 We herein propose a theoretically justified and generally applicable framework to estimate and
91 partition the phenotypic variance of reaction norms, towards three main goals: (i) quantify the contri-
92 bution of plasticity to the total phenotypic variance in reaction norms; (ii) evaluate the contribution
93 of different aspects of reaction norm shape, and of the full assumed reaction norm model, to overall
94 plastic phenotypic variation; and (iii) quantify heritable variation in the trait and its plasticity, due to
95 the different aspects of the reaction norm. We provide this framework as a new R package `Reacnorm`,
96 including a tutorial to guide users in applying it. Our hope is that this will stimulate more quantita-
97 tive investigations of the ways in which phenotypic plasticity contributes to phenotypic variation and
98 evolutionary change.

99 Reaction norm models

100 In the broadest sense, a reaction norm is a decomposition of phenotypic variation among known
101 (often controlled) versus unknown sources of environmental variation. In this sense, we can start by
102 decomposing the phenotypic trait z into two components:

$$z = \hat{z} + \tilde{z}. \quad (1)$$

103 The first term \hat{z} is the reaction norm, that is, the component of phenotypic variation that can be
104 predicted (hence the hat notation) from knowing both the genotype (which we will note g throughout)
105 of an individual and the environment (which we will note ε throughout) in which it developed. Note
106 that by “environment”, we mean either an experimentally controlled environmental variable, or a focal
107 variable (e.g. temperature) within a naturally occurring environmental context. The second term \tilde{z} is
108 the component of the measured phenotype that cannot be predicted from genotype and environment,
109 and arises from unknown environmental factors (usually described as micro-environmental variation),
110 developmental noise, and measurement error.

111 Types of reaction norms \hat{z} can be further categorised according to the type of environmental
112 variation. The environment may be inherently categorical and unordered, such as host plant for a
113 herbivore insect. It may be ordered but with no (or unknown) quantitative value, such as low, medium,
114 and high treatments. Or it may be ordered quantitatively, with values that are either intrinsically
115 discrete, such as habitat quality, or continuous, such as temperature or salinity.

Table 1: List of the main notations, as well as their source of variation. We here distinguish the “focal” environment, which only concerns the environmental variable used to parametrise the reaction norm, from other putative sources of environmental variation that may influence the phenotypic trait (sometimes described as micro-environmental variation). “Everything” in the table thus includes all (focal and other) sources of environmental and genetic variation, developmental noise and measurement error.

Notation	Explanation	Varies over
z	Phenotypic value for the trait	Everything
\hat{z}	Phenotype as predicted from the environment and the genotype	Focal environment, genotypes
ε	Environmental variable	—
$\boldsymbol{\mu}$	Vector of the average value of the phenotypic in each environment	Focal environment
\mathbf{G}_z	Additive genetic variance-covariance matrix of trait values across environments (character states)	—
$\boldsymbol{\theta}_g$	Vector of parameter values of the reaction norm for genotype g	Genotypes
$\boldsymbol{\theta}$	Vector of mean values of the reaction parameters over the genotypes	—
\mathbf{G}_θ	Additive genetic variance-covariance matrix of the reaction norm parameters	—
$\boldsymbol{\psi}_\varepsilon$	Reaction norm gradient, the vector of partial derivatives of the phenotype z against reaction norm parameters $\boldsymbol{\theta}_g$, averaged over the genotypes at environment ε	Focal environment
$\boldsymbol{\Psi}$	Variance-covariance matrix of $\boldsymbol{\psi}_\varepsilon$ across environments	—
V_P	Total phenotypic variance in the trait z	—
V_{Res}	Residual variance, not explained by the reaction norm	—
$V_{\text{Plas}}, P_{\text{RN}}^2$	Phenotypic variance arising from changes in the mean reaction norm across environments; divided by V_P for P_{RN}^2	—
$V_{\text{Gen}}, H_{\text{RN}}^2$	Total genetic variance in the trait across environments; divided by V_P for H_{RN}^2	—
$V_{\text{Add}}, h_{\text{RN}}^2$	Total additive genetic variance in the trait across environments; divided by V_P for h_{RN}^2	—
V_A, h^2	Marginal additive genetic variance of the trait, i.e. based on the mean breeding values across environments, divided by V_P for h^2	—
$V_{A \times E}, h_1^2$	Additive genetic variance in plasticity, i.e. variance of the mean-centred breeding values, divided by V_P for h_1^2	—
$\pi_{\text{Sl}}, \pi_{\text{Cv}}$	Proportion of V_{Plas} explained by the average slope (π_{Sl}) or curvature (π_{Cv}) of the average reaction norm	—
φ_i, φ_{ij}	Proportion of V_{Plas} explained by parameter i , or by covariation between parameter i and j for a polynomial reaction norm	—
γ_i, γ_{ij}	Proportion of V_{Add} explained by the additive genetic (co)variation in parameter i (and j)	—
l_i, l_{ij}	Proportion of $V_{A \times E}$ explained by the additive genetic (co)variation in parameter i (and j)	—

116 When environments are categorical, the reaction norm can be studied by treating phenotypic
117 values in different environments as alternative ‘character states’, considered as different traits in a
118 multivariate framework (Via & Lande 1985; Falconer 1952). The mean character state may differ
119 among environment if the trait is plastic; phenotypic and genetic variation may be larger in some
120 environments; and phenotypes may be more or less correlated across environments (Via & Lande
121 1985; Falconer 1952). Such a modelling framework is readily described by Equation 1 for a genotype
122 g and environment ε_k (where the index k is used to reflect the discrete aspect of the environmental
123 variable). In practice, such an approach would correspond to an ANOVA (or a mixed model) with

124 discrete environment and genotype-within-environment as (random) effects of the model. In its most
 125 compact form, such a statistical model can be framed as a multivariate Gaussian distribution, with a
 126 number of dimensions corresponding to the number of categories in the environment,

$$\hat{\mathbf{z}} \sim \mathcal{N}(\boldsymbol{\mu}, \mathbf{G}_z), \quad (2)$$

127 where $\boldsymbol{\mu}$ is the vector of expected phenotypic values (across genotypes) within each environment,
 128 and \mathbf{G}_z is the genetic variance-covariance matrix of trait values within and across environments. Note
 129 that when the environment is quantitative but discrete, one may still use the character-state approach,
 130 but structuring correlations in \mathbf{G}_z by environmental distance, in effect treating the phenotype as a
 131 stochastic process characterized by its autocovariance function across environments (Pletcher & Geyer
 132 1999).

133 For quantitative environments (both discrete and continuous), the most common approach is to
 134 model the reaction norm as a function of environment and genotype:

$$\hat{z} = f(\varepsilon, \boldsymbol{\theta}_g), \quad (3)$$

135 where ε is the environmental value, and $\boldsymbol{\theta}_g$ is a vector that contains the parameters of the function (e.g.
 136 coefficients associated to each exponent for a polynomial) for each genotype g ; these parameters are
 137 thus genetically variable. The parameters $\boldsymbol{\theta}_g$ are generally assumed to be polygenic and thus follow a
 138 multivariate Gaussian distribution,

$$\boldsymbol{\theta}_g \sim \mathcal{N}(\bar{\boldsymbol{\theta}}, \mathbf{G}_\theta), \quad (4)$$

139 where $\bar{\boldsymbol{\theta}}$ is the vector of average parameter values across genotypes and \mathbf{G}_θ is the additive genetic
 140 variance-covariance matrix of the parameters $\boldsymbol{\theta}_g$. This approach has been described alternatively as
 141 the “reaction norm” approach, the “polynomial approach”, or a parametric version of function-valued
 142 traits. To keep it general here and avoid confusion with the general concept of reaction norm as
 143 defined in Equation 1 (which applies even to categorical environments), we will describe it as the
 144 “curve-parameter” approach.

145 It can be shown that the character-state and curve-parameter approaches are equivalent, following
 146 the spirit of de Jong (1995), who showed that a polynomial curve of sufficient order is exactly equivalent
 147 to a character-state model. In particular, the character-state in Equation 2 can be expressed using
 148 Equation 3 and Equation 4 by letting $\bar{\boldsymbol{\theta}} = \boldsymbol{\mu}$, $\mathbf{G}_\theta = \mathbf{G}_z$ and f a function that outputs the k th value
 149 of $\boldsymbol{\theta}_g$ when evaluated at ε_k environment (see Appendix A). In the following, we will derive general
 150 results using the more general formalism of Equation 3 and Equation 4, and then express them for

151 the particular case of the character-state approach when relevant.

152 Partitioning variation in reaction norms

153 Complete partition of the variation in reaction norms

154 The total phenotypic variance in the reaction norm can be partitioned by isolating independent com-
155 ponents of variation. The main reasoning will be summarised here, with more mathematical details
156 provided in the [Appendix A](#) to [Appendix D](#). For a start, the terms in [Equation 1](#) are assumed to
157 be independent, such that the total phenotypic variance $V(z)$ (usually noted V_P) is the sum of the
158 variance predicted by the genotype and the environment $V(\hat{z})$, plus a residual component of variance
159 $V(\tilde{z}_i)$, which we will note V_{Res} . Then, a second distinction can be made between the general, average
160 shape of the reaction norm, and the genotype-specific variation surrounding such average, as illus-
161 trated in [Figure 1](#) using a quadratic reaction norm. The component of phenotypic variance arising
162 from plastic responses to the environment by the mean reaction norm, i.e. after averaging across all
163 genotypes ([Figure 1](#)), will be denoted V_{Plas} . This variance can be considered as fully ascribed to the en-
164 vironmental component of phenotypic variation. The component of phenotypic variation attributable
165 to genetic variation in the reaction norm [Figure 1](#) will be denoted V_{Gen} . As these two components
166 are independent by construction, denoting as $E_{g|\varepsilon}(\hat{z})$ the expected value of the reaction norm across
167 genotypes at a given environmental value ε , we have

$$V(\hat{z}) = V(E_{g|\varepsilon}(\hat{z})) + V(\hat{z} - E_{g|\varepsilon}(\hat{z})) = V_{\text{Plas}} + V_{\text{Gen}}, \quad (5)$$

168 such that

$$V_P = V_{\text{Plas}} + V_{\text{Gen}} + V_{\text{Res}}. \quad (6)$$

169 Compared to the classical equation $V_P = V_G + V_E + V_{G \times E}$ (Falconer & Mackay 1996; Lynch & Walsh
170 1998; Des Marais et al. 2013), the correspondence is that $V_E = V_{\text{Plas}} + V_{\text{Res}}$ and $V_{\text{Gen}} = V_G + V_{G \times E}$.
171 We have thus decomposed the environmental variance into a component due to phenotypic plasticity
172 in response to ε (V_{Plas}) on the one hand, and any other residual source of phenotypic variation (V_{Res})
173 on the other hand, as commonly done in theory (Via & Lande 1985; Gavrilets & Scheiner 1993b) as
174 well as in practice.

175 The genotypic variance V_{Gen} accounts for all sources of genetic variation, including the genotype-
176 by-environment interaction. Note that this contrasts with a view where the genotype-by-environment
177 interaction is instead associated with the environmental component, e.g. as *plastic variance* (Scheiner

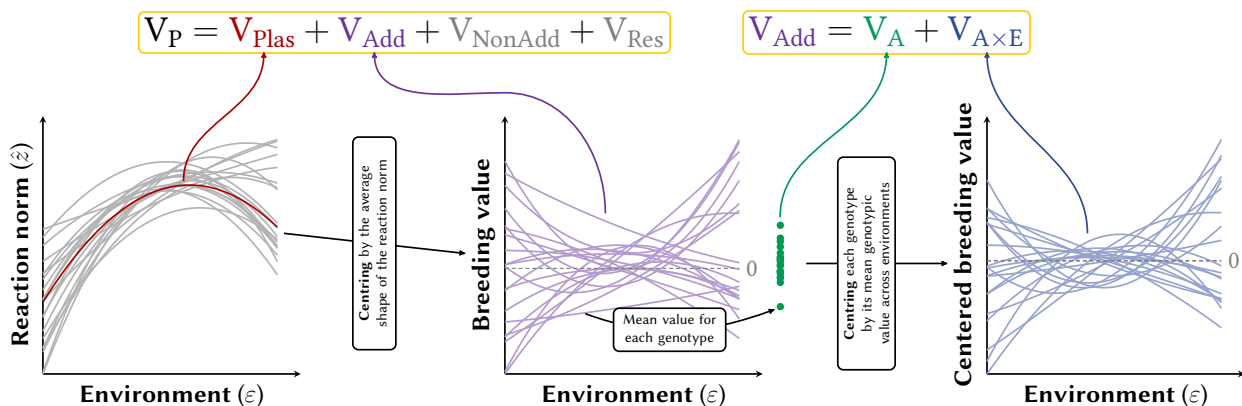


Figure 1: Illustration of the full variance decomposition using quadratic reaction norms. We start from the reaction norms (left graph, grey lines, the residual variance is not illustrated) and compute its average shape across all genotypes (left graph, red line). The phenotypic variance arising from this average shape is V_{Plas} . Centring the reaction norms along this average shape directly yields the distribution of the breeding values along environments (middle graph, purple lines), because in this quadratic case, the non-additive genetic variance is $V_{NonAdd} = 0$. The total variance of the breeding values along the environment is V_{Add} . The classical, average additive genetic variance V_A is the variance of the average of the breeding values across the environments for each genotype (middle graph, green dots). The $V_{A \times E}$ is the variance of the remainder of the breeding values after mean-centring (right graph, blue lines).

179 The genotypic variance V_{Gen} can be further decomposed in two steps. First, we can isolate the *addi-*
 180 *tive* genetic variance (V_{Add}), from the *non-additive* genetic variance (V_{NonAdd}) arising from dominance
 181 and epistasis (Lynch & Walsh 1998; Falconer & Mackay 1996). Usually, models like Equation 2 or
 182 Equation 4 are defined using additive genetic variance-covariance matrices for their basic parameters,
 183 meaning that V_{Add} can be directly estimated from the models. As such, we will discard explicit inclu-
 184 sion of dominance or epistasis variance components in a theoretical or statistical model throughout,
 185 for the sake of simplicity. However, non-additive genetic variance can still arise from non-linearity
 186 in the (assumed) developmental system (Rice 2004; Morrissey 2015; de Villemereuil et al. 2016; de
 187 Villemereuil 2018), meaning that non-additive variance can be generated by the reaction norm itself.
 188 Looking at Equation 3 and Equation 4, the ultimate source of any additive genetic variation in the
 189 trait z comes from the additive genetic variation in the parameters θ . As a result, non-additivity in
 190 the trait arises when the function $f(\epsilon, \theta)$ in Equation 3 is non-linear with regard to θ , a situation
 191 we will refer to as “non-linearity in the parameters”. Importantly, this means that polynomial (e.g.
 192 quadratic) functions, which are linear in their parameters, are such that $V_{NonAdd} = 0$ and $V_{Gen} = V_{Add}$.

193 When studying the evolution of plasticity, it proves useful to further decompose V_{Add} into two
 194 components. The first is the marginal additive genetic variance of the trait, arising from differences in
 195 average breeding values between genotypes, and typically equal to the classical V_A . In other words, V_A
 196 is the variance of the breeding values after averaging them across environments (Figure 1), as would

197 be obtained if the genotype-by-environment interaction was ignored altogether. For example, it would
 198 be the output of a simple animal model analysis of repeated measurements of a plastic trait in a wild
 199 population. The second component of V_{Add} is the additive genetic variance of plasticity, which we will
 200 note $V_{\text{A}\times\text{E}}$ (for additive genetic component due to genotype-by-environment interactions). $V_{\text{A}\times\text{E}}$ is
 201 the remaining additive genetic variance in the reaction norm after removing the mean breeding value
 202 for each genotype (Figure 1). This definition is akin to the one used by Albecker et al. (2022), but
 203 here more directly expressed in terms of variance of breeding values, i.e. additive genetic variance. It
 204 measures the potential for evolution of plasticity in the trait. Notably, if $V_{\text{A}\times\text{E}} = 0$ but $V_{\text{Add}} > 0$,
 205 then the additive genetic variation in the reaction norms is only due to average differences between
 206 genotypes, i.e. the reaction norms of different genotypes are parallel. The variances V_{A} and $V_{\text{A}\times\text{E}}$ are
 207 exactly equivalent to the classical decomposition using V_{G} and $V_{\text{G}\times\text{E}}$, only applied to the heritable
 208 part of the genetic variance. We show below that it is possible to express V_{Add} , V_{A} and $V_{\text{A}\times\text{E}}$ in a way
 209 that encompasses all approaches of reaction norm, from a character-state to a curve that is non-linear
 210 in its parameters, by computing reaction norm gradients of the trait z with respect to its reaction
 211 norm parameters θ , in line with previous theoretical results for the quantitative genetics of non-linear
 212 developmental systems and non-Gaussian traits (Morrissey 2015; de Villemereuil et al. 2016),.

213 The complete partition of the phenotypic variance is thus:

$$V_{\text{P}} = V_{\text{Plas}} + V_{\text{A}} + V_{\text{A}\times\text{E}} + V_{\text{NonAdd}} + V_{\text{Res}}. \quad (7)$$

214 From this, it is possible to derive unitless quantities of interest, for instance by standardising by the
 215 phenotypic variance. In particular:

$$P_{\text{RN}}^2 = \frac{V_{\text{Plas}}}{V_{\text{P}}}, \quad (8)$$

216 is the proportion of the phenotypic variance arising from average plastic responses to environments
 217 (depending on the average reaction norm shape). Variance-standardised additive genetic variances
 218 are heritabilities. In our case, we can use V_{Add} , V_{A} or $V_{\text{A}\times\text{E}}$ as the numerator, yielding the following
 219 relationship:

$$h_{\text{RN}}^2 = \frac{V_{\text{Add}}}{V_{\text{P}}} = \frac{V_{\text{A}}}{V_{\text{P}}} + \frac{V_{\text{A}\times\text{E}}}{V_{\text{P}}} = h^2 + h_{\text{I}}^2. \quad (9)$$

220 In other words, the heritability of the trait when fully accounting for its reaction norm (h_{RN}^2) is
 221 equal to the marginal heritability of the trait (h^2 , based on the averaged breeding values across
 222 environments) plus the heritability of plasticity, arising from interaction with the environment (h_{I}^2). If
 223 it is not possible to measure additive genetic variances due to limitations in the experimental design
 224 (e.g. when “genotypes” correspond to populations, accessions or clones), it is possible to perform the

225 same decomposition using “broad-sense heritabilities”,

$$H_{\text{RN}}^2 = \frac{V_{\text{Gen}}}{V_{\text{P}}} = \frac{V_{\text{G}}}{V_{\text{P}}} + \frac{V_{\text{G} \times \text{E}}}{V_{\text{P}}} = H^2 + H_{\text{I}}^2. \quad (10)$$

226 In all cases, the quantity:

$$T_{\text{RN}}^2 = \frac{V_{\text{Plas}} + V_{\text{Gen}}}{V_{\text{P}}} = P_{\text{RN}}^2 + H_{\text{RN}}^2 \quad (11)$$

227 would measure the proportion of the phenotypic variance explained by the (possibly plastic and ge-
 228 netically variable) reaction norm, and thus our ability to predict the individual phenotype from the
 229 genotype and the environment. In a linear context with respect to the parameters, when the environ-
 230 ment is considered a fixed quantity, the quantities P_{RN}^2 and T_{RN}^2 are analogous to the (resp. marginal
 231 and conditional) coefficient of determination of the reaction norm (Nakagawa & Schielzeth 2013; John-
 232 son 2014), but their definition here is given beyond that simple context. Importantly, so far we are
 233 not making any statement about the actual reaction norm shape: P_{RN}^2 captures the contribution of
 234 the average reaction norm regardless of its shape, and the broad- or narrow-sense heritabilities the
 235 contribution of various aspects the genetic variation to the phenotypic variance. The contribution of
 236 detailed aspects of reaction norms shape to phenotypic variation are obtained by further partitioning
 237 V_{Plas} and the additive genetic variances, as we do below.

238 Contributions of reaction norm shape and parameters to the plastic 239 variance

240 As stated in Equation 5, the general definition of the variance arising from the average reaction norm
 241 is $V_{\text{Plas}} = \text{V}(\text{E}_{g|\varepsilon}(\hat{z}))$. Important simplifications arise in more particular cases. For example, when
 242 the assumed curve is linear in its parameters, $\text{E}_{g|\varepsilon}(\hat{z}) = f(\varepsilon, \bar{\theta})$, where $\bar{\theta}$ is the average value of the
 243 parameters across genotypes. In particular, in the case of a quadratic reaction norm (Scheiner 1993a;
 244 Gavrillets & Scheiner 1993a; Morrissey & Liefting 2016):

$$f(\varepsilon, \theta_g) = (\bar{a} + a_g) + (\bar{b} + b_g)\varepsilon + (\bar{c} + c_g)\varepsilon^2, \quad (12)$$

245 where \bar{a} , \bar{b} , \bar{c} are the average intercept, first- and second-order parameters of the model, and a_g , b_g and
 246 c_g are genotype-specific deviation from these average values for the same parameters, we can express
 247 V_{Plas} simply as:

$$V_{\text{Plas}} = \bar{b}^2 \text{V}(\varepsilon) + \bar{c}^2 \text{V}(\varepsilon^2) + 2\bar{b}\bar{c}\text{cov}(\varepsilon, \varepsilon^2). \quad (13)$$

248 If the environmental variable ε has been mean-centred and is symmetrical, then $\text{cov}(\varepsilon, \varepsilon^2) = 0$ and
 249 the third term vanishes. Finally, in the case of a character-state model, the average phenotype in
 250 each environment ε_k is readily provided by the μ_k in [Equation 2](#), so that $V_{\text{Plas}} = V(\mu)$. Once V_{Plas} is
 251 computed, its standardised version P_{RN}^2 follows by dividing by the total phenotypic variance.

252 Pushing the analysis further, we aim to compute the contributions of different aspect of reaction
 253 norm shape to the overall environmental plastic variance of the trait, notably the contribution of its
 254 slope and curvature, which we will denote as π_{Sl} and π_{Cv} , respectively. For this, at least one of two
 255 of the following assumptions must valid: (i) ε follows a normal distribution, or (ii) the true reaction
 256 norm is quadratic. In all cases, it also require that the environmental variable has been mean-centered.
 257 A last requirement is for f to be at least twice differentiable with respect to ε (which excludes e.g.
 258 the character-state approach). In this case, these terms simply depend on the average first- and
 259 second-order derivative of $E_{g|\varepsilon}(\hat{z})$ and the variance of ε and ε^2 (see [Appendix D1](#)):

$$\pi_{\text{Sl}} = \frac{E\left(\frac{dE_{g|\varepsilon}}{d\varepsilon}(\hat{z})\right)^2 V(\varepsilon)}{V_{\text{Plas}}}, \quad \pi_{\text{Cv}} = \frac{\frac{1}{4}E\left(\frac{d^2E_{g|\varepsilon}}{d\varepsilon^2}(\hat{z})\right)^2 V(\varepsilon^2)}{V_{\text{Plas}}}. \quad (14)$$

260 An important point arising from [Equation 14](#) is that the relative importance of variation in the slope
 261 and curvature components of reaction norm depend on variation in the environment, respectively
 262 $V(\varepsilon)$ and $V(\varepsilon^2)$. Crucially, we chose to express this partitioning using the mean environment as the
 263 reference environment (as commonly practiced, e.g. [Morrissey & Liefting 2016](#)), but any other choice
 264 of a reference environment would result in a different π -partition, notably due to a non-null value for
 265 $\text{Cov}(\varepsilon, \varepsilon^2)$. Fortunately, neither V_{Plas} nor P_{RN}^2 are impacted by this choice in the reference environment.
 266 Furthermore, if the reaction norm is linear on the parameters, the derivatives of $E_{g|\varepsilon}(\hat{z})$ can be directly
 267 taken as the derivatives of f . In particular, for a quadratic reaction norm as in [Equation 12](#), for a
 268 mean-centred environment, those quantities simply are:

$$\pi_{\text{Sl}} = \frac{\bar{b}^2 V(\varepsilon)}{V_{\text{Plas}}}, \quad \pi_{\text{Cv}} = \frac{\bar{c}^2 V(\varepsilon^2)}{V_{\text{Plas}}}, \quad (15)$$

269 consistent with the fact the first and second order coefficients of a quadratic polynomial correspond
 270 to its average slope and curvature, respectively. Only in this configuration do we have $\pi_{\text{Sl}} + \pi_{\text{Cv}} = 1$.
 271 Unfortunately, this simple, geometric interpretation of the polynomial coefficients is lost above the
 272 second-order case (see [Appendix D](#)).

273 [Figure 2](#) shows the values of π_{Sl} and π_{Cv} for various quadratic reaction norms, assuming ε follows
 274 either a normal or uniform distribution, with same mean 0 and variance 1. The values for π_{Sl} and
 275 π_{Cv} translate well the perceived “trendiness” (for large π_{Sl}) or “curviness” (for large π_{Cv}) of reaction

276 norms, but they may also strongly depend on the statistical distribution of the environmental variable
 277 ε , as shown especially in the third example of Figure 2. In this example, the difference arises because
 278 the assumed environmental distributions have different kurtosis (the scaled fourth central moment,
 279 related to $V(\varepsilon^2)$ in Equation 15). Because $V(\varepsilon^2)$ is larger for the Gaussian, this distribution leads to
 280 larger π_{Cv} than the uniform.

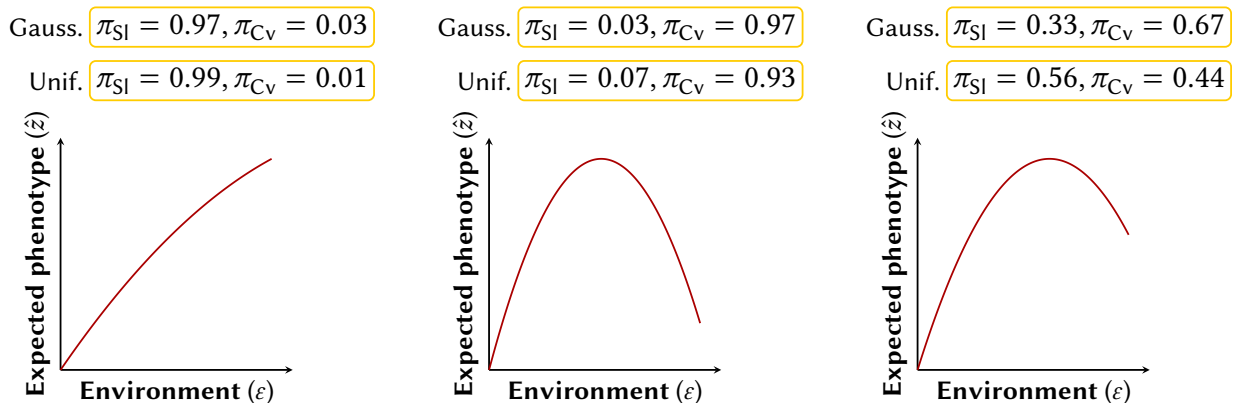


Figure 2: Computation of $\pi_{Sl} = \pi_b$ and $\pi_{Cv} = \pi_c$, the relative contributions of linear and quadratic terms to phenotypic variation caused by the mean reaction norm, for different shapes of reaction norms, and two distributions of the environmental variable ε : a standard Gaussian (of mean 0 and variance 1), and a uniform distribution between $-\sqrt{3}$ and $\sqrt{3}$ (of mean 0 and variance 1).

281 When it is not possible to assume that ε is normally distributed (because it is discrete, or experi-
 282 mentally constrained) and a quadratic assumption is not a good fit to the reaction norm, it is always
 283 possible to use a higher-order polynomial model to approximate the true reaction norm, in line with
 284 theoretical work by de Jong (1990), Gavrillets & Scheiner (1993a), and de Jong (1995). In this case, we
 285 can conduct an alternative decomposition based on the parameters of the polynomial (rather than the
 286 mean slope and curvature of the function). To distinguish this parameter-based decomposition from
 287 the specific decomposition in terms of slope and curvature, we use a different notation. The relative
 288 contribution of a given exponent m in the polynomial to the variance caused by the mean plasticity
 289 becomes (see Appendix D2)

$$\varphi_m = \frac{\bar{\theta}_m^2 V(\varepsilon^m)}{V_{Plas}}, \quad (16)$$

290 and the contribution of the covariance between exponents l and m is

$$\varphi_{lm} = \frac{2\bar{\theta}_l\bar{\theta}_m \text{Cov}(\varepsilon^l, \varepsilon^m)}{V_{Plas}}. \quad (17)$$

291 Note that even with a symmetrical and mean-centred environment, the covariance between higher-
 292 order exponents will not be zero in general, contrary to ε and ε^2 in the quadratic case. Using orthogonal
 293 polynomials would solve this issue of covariances, but at the cost of a more complex interpretation of

294 the coefficients. More generally, this φ -decomposition only relies on the assumption that the reaction
 295 norm is linear on its parameters, which includes polynomials as a particularly useful special case.
 296 We summarise the requirements and applications for the π - and φ -decomposition depending on the
 297 context in [Figure 3](#).

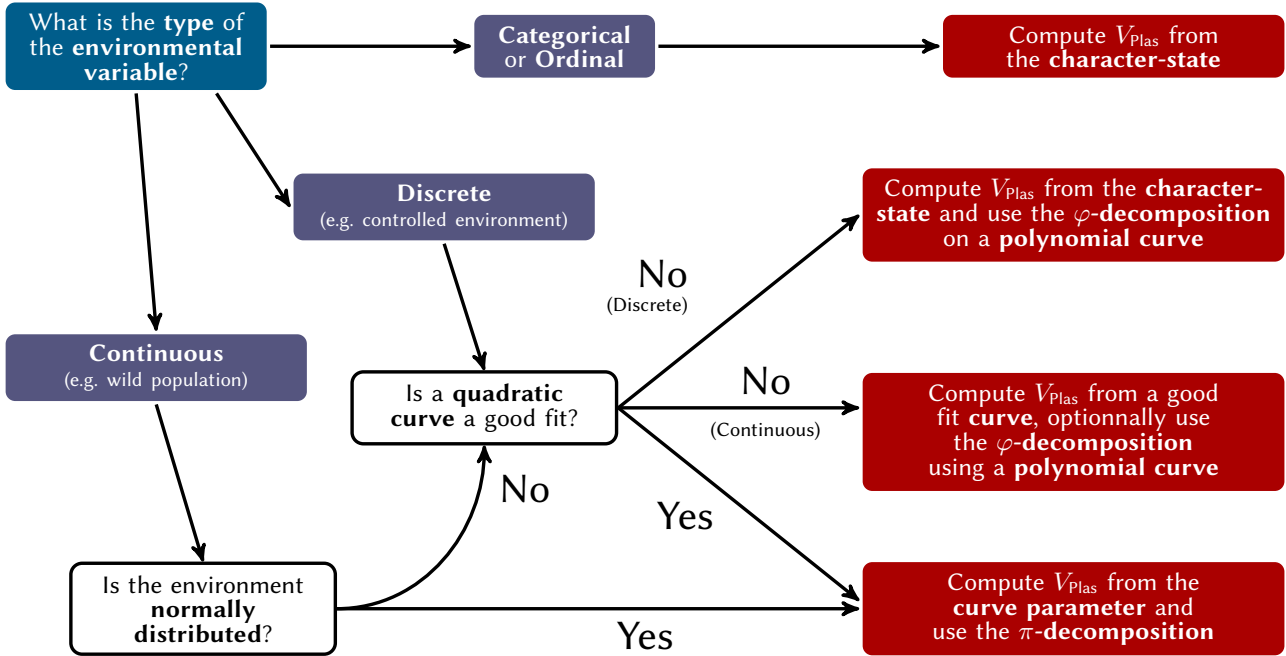


Figure 3: Decision tree summarising our suggested workflow for the computation and decomposition of V_{Plas} , depending on the nature of the environmental variable, its normality and the validity of a quadratic approximation of the reaction norm shape.

298 Contributions of reaction norm parameters to the genetic variance

299 We can expression the variance of the genotypic values of the reaction norms in [Equation 5](#) in a slightly
 300 different, but more operational, manner:

$$V_{Gen} = V(\hat{z} - E_{g|\varepsilon}(\hat{z})) = E(V_{g|\varepsilon}(\hat{z})), \quad (18)$$

301 i.e. the total genotypic variance of the reaction norms is equal to the environment-specific genotypic
 302 variance averaged across environments. From an evolutionary perspective, the component of main
 303 interest is rather the total additive genetic variance of the reaction norm V_{Add} , which will be the main
 304 focus of this section. As a reminder, we here assume, that the experimental design allows for the
 305 inference of the additive genetic variance of the parameters of the reaction norm (\mathbf{G}_z or \mathbf{G}_θ above),
 306 and that non-additive variance in the trait V_{NonAdd} only arises when the reaction norm is non-linear
 307 in the parameters (i.e. dominance and/or epistasis were not fitted in the statistical model). This

308 assumption is for the sake of simplicity, as our framework can include such effects into V_{Gen} if needed.

309 A general way to relate the additive genetic variance of the trait to the additive genetic variances
 310 of the reaction norm parameters is through a vector that we describe as the reaction norm gradient,
 311 which we will note $\boldsymbol{\psi}_\varepsilon$ (following notations in de Villemereuil et al. 2016),

$$\boldsymbol{\psi}_\varepsilon = \text{E}_g \left(\frac{\partial z}{\partial \boldsymbol{\theta}} \right)_\varepsilon, \quad (19)$$

312 where the subscript ε makes it clear that $\boldsymbol{\psi}_\varepsilon$ will generally be a function of the environment. In the
 313 case of a quadratic curve, $\boldsymbol{\psi}_\varepsilon$ is the $(1, \varepsilon, \varepsilon^2)^T$ vector (see [Appendix C3](#) for a polynomial of arbitrary
 314 order). In the case of a character-state model, $\boldsymbol{\psi}_{\varepsilon_k}$ is a vector with 1 for the k th environmental level
 315 (or character state), and zero elsewhere. Whether or not the reaction norm is linear in its parameters,
 316 the additive genetic variance of the trait in a given environment ε is (Morrissey 2015; de Villemereuil
 317 et al. 2016, and see [Appendix B](#)),

$$V_{A|\varepsilon} = \boldsymbol{\psi}_\varepsilon^T \mathbf{G}_\theta \boldsymbol{\psi}_\varepsilon, \quad (20)$$

318 where superscript T denotes matrix transposition, \mathbf{G}_θ the genetic covariance matrix of reaction norm
 319 parameters as defined in [Equation 4](#) for the curve-parameter approach, and \mathbf{G}_θ is \mathbf{G}_z from [Equation 2](#)
 320 for the character-state approach. The total additive genetic variance in the reaction norm, V_{Add} , is
 321 the average of $V_{A|\varepsilon}$ across environments (see [Appendix C1](#)):

$$V_{\text{Add}} = \text{E}(\boldsymbol{\psi}_\varepsilon^T \mathbf{G}_\theta \boldsymbol{\psi}_\varepsilon). \quad (21)$$

322 The marginal additive genetic variance of the trait V_A , based on breeding values averaged across
 323 environments, is (see [Appendix C2](#))

$$V_A = \text{E}(\boldsymbol{\psi}_\varepsilon)^T \mathbf{G}_\theta \text{E}(\boldsymbol{\psi}_\varepsilon) \quad (22)$$

324 The additive genetic variance in plasticity is thus (see [Appendix C2](#)):

$$V_{A \times E} = V_{\text{Add}} - V_A = \text{E}(\boldsymbol{\psi}_\varepsilon^T \mathbf{G}_\theta \boldsymbol{\psi}_\varepsilon) - \text{E}(\boldsymbol{\psi}_\varepsilon)^T \mathbf{G}_\theta \text{E}(\boldsymbol{\psi}_\varepsilon). \quad (23)$$

325 If we define $\boldsymbol{\Psi} = \text{E}(\boldsymbol{\psi}_\varepsilon \boldsymbol{\psi}_\varepsilon^T) - \text{E}(\boldsymbol{\psi}_\varepsilon) \text{E}(\boldsymbol{\psi}_\varepsilon)^T$, the variance-covariance matrix of the reaction norm
 326 gradients across environments, then a more intuitive way to express $V_{A \times E}$ is as a sum, for all pairs of
 327 parameters, of the (co)variance of their reaction norm gradient across environments (in $\boldsymbol{\Psi}$) and their

328 additive genetic (co)variance (in \mathbf{G}_θ):

$$V_{A \times E} = \sum_{i,j} \Psi_{(i,j)} \mathbf{G}_{\theta(i,j)} = \text{Tr}(\Psi \mathbf{G}_\theta), \quad (24)$$

329 where Tr is the trace of a matrix. All of the quantities above can be divided by V_P to get the
330 corresponding heritabilities.

331 To illustrate with an example, for a quadratic reaction norm with mean-centred environment as
332 shown in [Figure 1](#), $\psi_\varepsilon = (1, \varepsilon, \varepsilon^2)$ and thus we have (see [Appendix C3](#))

$$\begin{aligned} V_{\text{Add}} &= V_a + (V_b + 2C_{ac})\text{E}(\varepsilon^2) + V_c\text{E}(\varepsilon^4), \\ V_A &= V_a + 2C_{ac}\text{E}(\varepsilon^2) + V_c\text{E}(\varepsilon^2)^2, \\ V_{A \times E} &= V_b\text{V}(\varepsilon) + V_c\text{V}(\varepsilon^2), \end{aligned} \quad (25)$$

333 where V_a , V_b and V_c are the additive genetic variances in the parameters a_g , b_g and c_g , and C_{ac}
334 is the additive genetic covariance between the intercept a_g and the second-order effect c_g . Those
335 expressions are reminiscent of classical results from the theory of evolution of plasticity (e.g. de Jong
336 1990; Gavrillets & Scheiner 1993a), especially regarding the crucial role of C_{ac} in the evolution of
337 quadratic reaction norms, but here distinguishing three important components of the additive genetic
338 variance of reaction norms. In particular, we see how the additive genetic variance in plasticity, $V_{A \times E}$,
339 can be simply expressed as the sum of the products of the variances in the reaction norm gradients
340 (here the environment and its squared value) and the corresponding additive genetic variance in the
341 parameters (here b_g and c_g in [Equation 12](#)). This means that, in the quadratic case, genetic variances
342 in slope and curvature directly translate into variance in plasticity, as they should. By contrast, V_A
343 does not solely depend on the variance in the intercept V_a , but also on the quadratic coefficient, more
344 specifically its covariance with the intercept.

345 The expressions for these variance components in the character-state approach are best described
346 directly from the \mathbf{G}_z matrix. The total additive genetic variance along the reaction norm, V_{Add} , is the
347 average of the additive genetic variance in each environment, i.e. the average of the diagonal elements of
348 the \mathbf{G}_z . The marginal additive genetic variance of the trait, V_A , is the average of all the elements of the
349 \mathbf{G}_z matrix. Finally, the variance $V_{A \times E}$ is the sum of the products of the (co)variances in the frequency
350 of each environment and the additive genetic (co)variances in \mathbf{G}_z . We illustrate in [Appendix C4](#)
351 the relationship between the structure in the \mathbf{G}_z matrix and the additive genetic variances, but a
352 simplified statement is that $V_{A \times E} > 0$ as soon as the correlation between environments are different
353 from 1 or variances in the diagonal are not all equal.

354 To further decompose genetic variation in the reaction norms, we first note that here, the reaction
 355 norm parameters are the focus of the decomposition, rather than shape characteristics like the slope
 356 or curvature (with the exception of a quadratic reaction norm, the only case where they are formally
 357 linked). Because Equation 21 is a sum of products, and since G_θ is a constant, we can isolate each
 358 term of the resulting sum as:

$$\gamma_i = \frac{\mathbf{E}_\varepsilon(\psi_{\varepsilon,i}^2) V_g(\theta_i)}{V_{\text{Add}}}, \quad \gamma_{ij} = \frac{2\mathbf{E}_\varepsilon(\psi_{\varepsilon,i}\psi_{\varepsilon,j}) \text{Cov}_g(\theta_i, \theta_j)}{V_{\text{Add}}}, \quad \sum_i \gamma_i + \sum_{i<j} \gamma_{ij} = 1. \quad (26)$$

359 Here, γ_i provides the contribution of the i th parameter in the model to the total additive genetic
 360 variance V_{Add} , while γ_{ij} provides the contribution of the covariation between parameters i and j to
 361 V_{Add} . As such, this “ γ -decomposition” (where gamma refers to g for Genetics) measures the relative
 362 importance of genetic variances and covariances of the parameters to the evolvability of the plastic
 363 trait. Large values of γ_i indicate that genetic variation in the i th parameter translate into a large
 364 proportion of the genetic variation in the trait. Also, large positive or negative values for γ_{ij} indicate
 365 that covariation between parameters i and j can have a large impact in increasing or reducing genetic
 366 variation in the trait.

367 It is also possible to focus on the additive genetic variation in plasticity, $V_{\text{A} \times \text{E}}$, rather than the
 368 reaction norm itself, which yields:

$$\iota_i = \frac{\mathbf{V}(\psi_{\varepsilon,i}) V_g(\theta_i)}{V_{\text{A} \times \text{E}}}, \quad \iota_{ij} = \frac{2\text{Cov}_\varepsilon(\psi_{\varepsilon,i}, \psi_{\varepsilon,j}) \text{Cov}_g(\theta_i, \theta_j)}{V_{\text{A} \times \text{E}}}, \quad \sum_i \iota_i + \sum_{i<j} \iota_{ij} = 1. \quad (27)$$

369 This “ ι -decomposition” (where iota refers to i for Interaction) highlights the fact that $V_{\text{A} \times \text{E}}$ is the sum
 370 of the products of (co)variances in elements of the reaction norm gradient ψ_ε and the additive genetic
 371 (co)variances in the parameters.

372 For a quadratic reaction norm as in Equation 12 with a mean-centred environment, this yields:

$$\gamma_a = \frac{V_a}{V_{\text{Add}}}, \quad \gamma_b = \frac{V_b \mathbf{E}(\varepsilon^2)}{V_{\text{Add}}}, \quad \gamma_c = \frac{V_c \mathbf{E}(\varepsilon^2)^2}{V_{\text{Add}}}, \quad \gamma_{ac} = \frac{2C_{ac} \mathbf{E}(\varepsilon^2)}{V_{\text{Add}}}, \quad \iota_b = \frac{V_b \mathbf{V}(\varepsilon)}{V_{\text{A} \times \text{E}}}, \quad \iota_c = \frac{V_c \mathbf{V}(\varepsilon^2)}{V_{\text{A} \times \text{E}}}. \quad (28)$$

373 Note that since the environment has been mean-centred, we have $\mathbf{V}(\varepsilon) = \mathbf{E}(\varepsilon^2)$ since $\mathbf{E}(\varepsilon)^2 = 0$, and
 374 thus $\gamma_b = \iota_b$, i.e. in the quadratic case, all of the genetic variation in the slope contributes to the
 375 genetic variance in plasticity. Note also that genetic variance in reaction norm intercept a does not
 376 contribute to the heritability of plasticity ($\iota_a = 0$).

377 For the character-state, such decomposition can be performed but yields as many parameters as
 378 there are environments for γ , and pairwise combinations of environments for ι . They directly depend on

379 the additive genetic variance in each environment, weighed by its frequency in the experimental setting
 380 for γ ; and on the product between the (co)variance in frequency of the environment and the additive
 381 genetic (co)variance in or between environments for ι . While these quantities can be informative about
 382 particular (couple of) environment (e.g. large γ_k would sign that the k th environment is associated
 383 with a large genetic variance, compared to the others), they are certainly not summary quantities of
 384 the \mathbf{G}_z matrix and are difficult to easily relate to evolvability and constraints on reaction norms shape.
 385 The variances V_{Add} , V_{A} and $V_{\text{A}\times\text{E}}$ are more interesting summary statistics in this particular context.
 386 Another interesting summary quantity can be provided by the toolbox of multivariate quantitative
 387 genetics. Following (Kirkpatrick 2009), we can define the effective number of character states as

$$n_e = \sum_i \frac{\lambda_i}{\lambda_1}, \quad (29)$$

388 where λ_i is the i^{th} eigenvalue of \mathbf{G}_z ranked by size (i.e., λ_1 is the largest eigenvalue). Large n_e close
 389 to the actual number of assayed environments means that genetic variance is well balanced and little
 390 correlated across environments. Conversely, n_e near 1 means that most genetic variation lies along a
 391 single combination of character states, such that reaction norm evolution is highly constrained, i.e. the
 392 genetic correlations are very high between the environments. However, it would be wrong to equate
 393 $n_e = 1$ with an absence of genetic variance in plasticity: if the genetic variances within environments
 394 (i.e. the diagonal elements of \mathbf{G}_z) are variable while $n_e = 1$, this results in more evolvability in some
 395 environments, thus $V_{\text{A}\times\text{E}} > 0$. Reciprocally, a maximal value for n_e (i.e. equal to the number of
 396 environments) does not mean that the genetic variance in plasticity is maximised at the expense of
 397 additive genetic variance in the trait: for example, when there is no genetic covariances between
 398 environments and equal genetic variances within environments, n_e is maximised, but V_{A} is not zero.
 399 As a result, a combined interpretation of n_e and the ratio $V_{\text{A}\times\text{E}}/V_{\text{Add}}$ (i.e. how much of the total
 400 genetic variance in the reaction norm consists of genetic variance in plasticity) generates an interesting
 401 summary of the main properties of the \mathbf{G}_z matrix in the context of a character-state.

402 **Parameter estimation and variance partitioning in practice**

403 **Estimating the parameters**

404 All the parameters mentioned in the previous section can be estimated through commonly used sta-
 405 tistical frameworks. For the character-state approach (Equation 2), a random-intercept model can
 406 be used, or alternatively a “multi-trait” model (Rovelli et al. 2020; Mitchell & Houslay 2021). We

407 will focus here on the former, which is more easily implemented while seemingly scarcely used in the
408 literature on plasticity. In a random-intercept model, the environment is considered as a categorical
409 variable, to which a random effect is added using the genotype as the grouping factor. In the curve-
410 parameter approach, the appropriate models will be random-slope models for a polynomial approach
411 (as mentioned in Morrissey & Liefting 2016), or non-linear mixed models, fitting the reaction norm
412 function $f(\varepsilon, \boldsymbol{\theta})$ to the data. Random effects are fitted to the parameters of this function (with the
413 genotype as grouping factor), e.g. the intercept, slope, and any higher-order effects for a polynomial
414 function.

415 Since the parameters are estimated with noise, it is important to account for the impact of es-
416 timation uncertainty when computing variance components. In particular, while variances directly
417 obtained using random effects (e.g. genetic variances) are expected to be unbiased, the variances aris-
418 ing from fixed effects (e.g. variances related to V_{Plas}) should be corrected for biases due to uncertainty
419 (as the adjusted R^2 does for example). Details are provided in [Appendix E](#).

420 To compute the total phenotypic variance required to get the estimates \hat{P}_{RN}^2 , \hat{H}_{RN}^2 and \hat{h}_{RN}^2 , we
421 advise using the sum of all estimated components rather the raw sample variance. The former is
422 common practice in most quantitative genetics inference to account for potential imbalance in the
423 experimental or sampling design (Wilson et al. 2010; de Villemereuil et al. 2018).

424 We provide an R package, named Reacnorm github.com/devillemereuil/Reacnorm, providing func-
425 tions implementing the variance decomposition based on raw outputs of statistical models. A tuto-
426 rial is shipped with the package, as an R vignette, showing how to implement such models using the
427 Bayesian brms R packages (Bürkner 2017), along with Reacnorm.

428 Perfect modelling of quadratic curves

429 We simulated phenotypic data conforming to a quadratic reaction norm, to evaluate the performance
430 of the proposed approach when the reaction norm truly is quadratic. We considered both a discrete
431 and continuous environment. For the discrete environment, we considered $N_{\text{Gen}} = 20$ or 5 different
432 genotypes and an environmental gradient of $N_{\text{Env}} = 10$ or 4 values, equally spaced from -2 to 2. We
433 sampled $N_{\text{Rep}} = N_{\text{Gen}}$ individual measures for each genotype with a residual variance $V_{\text{Res}} = 0.25$. For
434 the continuous environment, we drew $N_{\text{Env}} = 10$ or 4 values from a normal distribution for each of the
435 $N_{\text{Gen}} = 200$ or 50 genotypes. Residual noise was applied around each measure for each genotype with
436 a residual variance $V_{\text{Res}} = 0.25$. In all cases, we defined a quadratic curve with average parameters
437 $\bar{\boldsymbol{\theta}} = (1.5, 0.5, -0.5)$ for intercept, slope and curvature. We then drew N_{Gen} different genotype-specific
438 vectors of curve-parameter $\boldsymbol{\theta}$ from a multivariate normal distribution with mean $\bar{\boldsymbol{\theta}}$ and (genotypic)

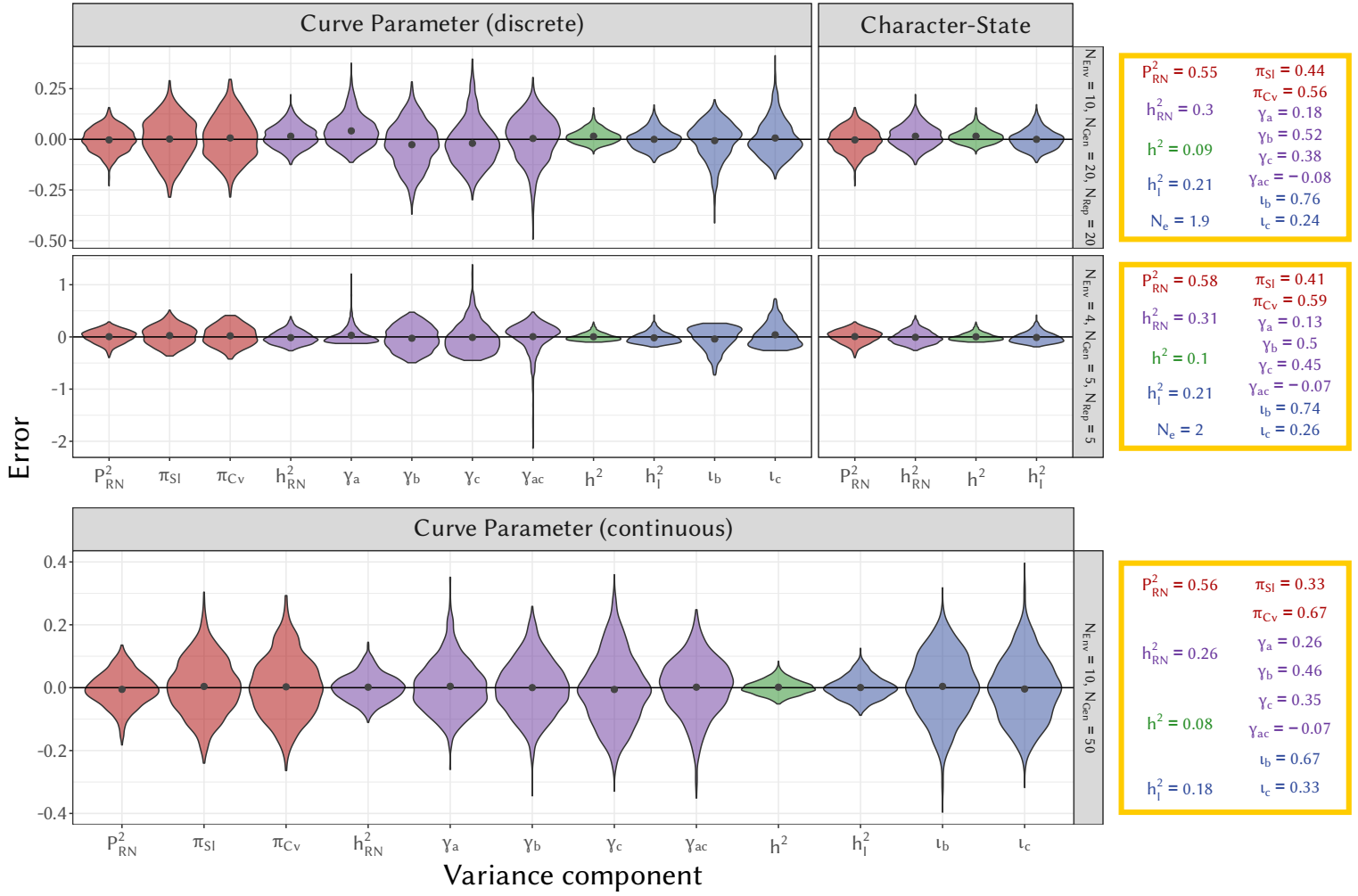


Figure 4: Distribution of the error (difference between the inferred and true value) for each the inferred variance components for three scenarios: two discrete (N_{env} : number of environments, N_{Gen} : number of different genotypes, N_{Rep} : number of replicates per genotype) and one continuous (N_{env} : number of environment tested per genotype, N_{Gen} : number of different genotypes). The grey dots correspond to the average over the 1000 simulations. The character-state approach was impossible for the continuous environment scenario. The yellow boxes on the right show the estimates for \hat{P}_{RN}^2 (proportion of variance generated by the plasticity in the mean reaction norm), \hat{h}_{RN}^2 (total heritability of the reaction norm), \hat{h}^2 (heritability based on average breeding values) and \hat{h}_1^2 (heritability of plasticity) for both the curve-parameter and character-state approaches. For the curve-parameter, the π -decomposition of \hat{P}_{RN}^2 into π_{SI} (contribution of the slope) and π_{Cv} (contribution of the curvature); the γ -decomposition of \hat{h}_{RN}^2 into γ_a (genetic contribution of the intercept), γ_b (genetic contribution of the slope), γ_c (genetic contribution of the curvature) and γ_{ac} (genetic contribution of the covariance between the intercept and the curvature) and the ι -decomposition of \hat{h}_1^2 into ι_b (slope) and ι_c (curvature) are also shown. The effective number of dimensions n_e from the character-state is not shown, due to an important bias impacting the comparison with the other parameters.

439 variance-covariance matrix

$$\mathbf{G}_\theta = \begin{pmatrix} 0.090 & -0.024 & -0.012 \\ -0.024 & 0.160 & 0.008 \\ -0.012 & 0.008 & 0.040 \end{pmatrix}.$$

440 **Figure 1** displays examples of curves resulting from these parameters. The simulation process was
 441 repeated 1000 times for each scenario, and for each simulated dataset, we ran estimations using the
 442 lme4 R package (Bates et al. 2015) under the curve-parameter (for discrete and continuous environ-

443 ment) and character-state (only for discrete environment) approaches, in order to check how these
 444 approaches compare in practice.

445 From the curve-parameter models, we computed \hat{V}_{Plas} (accounting for the uncertainty in fixed
 446 effects), then \hat{P}_{RN}^2 . We also computed the π -decomposition ($\hat{\pi}_{\text{SI}}$ and $\hat{\pi}_{\text{CV}}$, Equation 14), since the true
 447 reaction norm is quadratic here, as well as \hat{h}_{RN}^2 , \hat{h}^2 and \hat{h}_{I}^2 as in Equation 9. We then applied the
 448 γ -decomposition to \hat{h}_{RN}^2 (Equation 26): $\hat{\gamma}_a$ (impact of the genetic variation of the intercept), $\hat{\gamma}_b$ (for
 449 the slope), $\hat{\gamma}_c$ (for of the curvature) and $\hat{\gamma}_{ac}$ (for the covariance between the intercept and curvature).
 450 Similarly, we applied the ι -decomposition to h_{I}^2 (Equation 27): ι_b (for the slope) and ι_c (for the
 451 curvature). From the character-state model, we computed only \hat{P}_{RN}^2 , \hat{h}_{RN}^2 , \hat{h}^2 and \hat{h}_{I}^2 .

452 The yellow boxes in Figure 4 display the theoretical expected values for the different parameters
 453 for three scenarios of environmental variation (two discrete, one continuous; other scenarios are shown
 454 in Appendix F). Using the first discrete scenario as a reference for now, most of the total phenotypic
 455 variance comes from the average plasticity ($P_{\text{RN}}^2 = 0.55$). This, in turns, includes a large contribution
 456 from the curvature ($\pi_{\text{CV}} = 0.56$) of the average reaction norm, more than from its slope ($\pi_{\text{SI}} = 0.44$).
 457 The total heritability of the reaction norm is substantial ($h_{\text{RN}}^2 = 0.3$), but interestingly most of it
 458 is due to the heritability of plasticity ($h_{\text{RN}}^2 = 0.21$), while the marginal heritability of the trait is
 459 only $h^2 = 0.08$. Contrary to the average shape, most of the additive genetic variation comes from
 460 the slope, both when considering the total reaction norm ($\gamma_b = 0.52$), or plasticity alone ($\iota_b = 0.76$).
 461 All scenarios share the same underlying parameters θ and \mathbf{G}_θ , resulting in very comparable values
 462 for our variance decomposition (i.e. P_{RN}^2 and the heritabilities) across the different environmental
 463 sampling scheme. By contrast, the environmental sampling scheme (especially discrete v. continuous
 464 distribution) can substantially impact the expected values of the π -, γ - and ι -decompositions. This is
 465 especially true when switching from the discrete to the continuous scenarios (e.g. $\pi_{\text{SI}} = 0.44$ for the first
 466 discrete scenario while $\pi_{\text{SI}} = 0.33$ for the continuous scenario). Interestingly, the theoretical effective
 467 number of environment n_e is very stable when comparing the first (4 environments) and second (10
 468 environments) discrete scenarios ($n_e = 2$ v. $n_e = 1.9$), which is due to the constraining shape of the
 469 quadratic reaction norm.

470 Switching to the error in the estimation of the parameters (left panels of Figure 4), we see first
 471 that both the character-state and curve-parameter approaches allow for unbiased inference (Wilcoxon's
 472 rank test, $p > 0.05$), apart from a slight bias in the heritabilities (\hat{h}_{RN}^2 , \hat{h}^2 and \hat{h}_{I}^2) and some of their
 473 γ and ι components in the discrete scenarios ($< 5\%$ relative bias, Wilcoxon's rank test, $p < 0.05$),
 474 notably due to a slight overestimation of the genetic variance of the intercept (visible in the top row
 475 of Figure 4). A notable exception, not shown in the graphics of Figure 4, was the effective number of

476 dimensions, n_e , for the character-state. The relative bias was between -12% and -35% (Wilcoxon’s
 477 rank test, $p < 0.05$), and was mainly explained by an overestimation of the dominant eigenvalue
 478 λ_1 in Equation 29. For the discrete case, the precision of the estimates was not much influenced
 479 by the number of environments and depended more on the number of genotypes (see Figure S1).
 480 For the continuous case, both the number of environments and genotypes influenced the precision
 481 of estimates (see Figure S2). As a sanity check, we also verified that \hat{V}_{Tot} (not shown in Figure 4)
 482 reflected the raw phenotypic variance with extreme precision (correlation $> 99\%$) in the discrete case
 483 and very good precision (correlation $> 87\%$) in the continuous case. The difference between these
 484 two types of scenarios is explained by how the stochasticity in environmental values differs among
 485 them. Importantly, the results in Figure 4) also illustrate the exact equivalence, in the discrete case,
 486 between the curve-parameter and character-state approaches, as the distributions of \hat{P}_{RN}^2 and \hat{h}_{RN}^2
 487 were nearly identical (Figure 4, correlation $> 99\%$) between the two approaches. This means that
 488 our variance partitioning is not impacted by which approach is chosen to study plasticity, as long
 489 as the curve-parameter approach captures the true reaction norm shape. When this does not hold,
 490 the differences between estimates from these alternative approaches can be exploited efficiently, as we
 491 describe below.

492 Imperfect modelling of a non-polynomial reaction norm

493 The true shapes of reaction norms are generally unknown and may be complex, such that any curve-
 494 parameter model is likely to be mis-specified to some extent. In the case of a discrete environment, the
 495 character-state approach is arguably more general, as it does not assume anything about the “true”
 496 shape of the reaction norm (as pointed out previously by de Jong 1995). Nonetheless, having access
 497 to curve-parameters is often very interesting and more actionable (even in cases where the linear
 498 and quadratic components cannot be interpreted as the average slope and curvature), especially to
 499 predict evolution of phenotypic plasticity (see also de Jong 1995). To get the best of both worlds,
 500 we rely on the ability of the character-state approach to recover P_{RN}^2 , using it as an “anchor”, to
 501 assess the performance of a given curve. Note that, under these circumstances, it is not possible to
 502 obtain the most natural π -decomposition in Equation 14, so we instead rely on the φ -decomposition
 503 in Equation 16 (here taken at the second order). Because of this, we need to assess how “bad” our
 504 simplification using an imperfect curve is. To do so, we compute the ratio of the variance modelled
 505 by the polynomial curve to the total variance due to phenotypic plasticity:

$$M_{\text{Plas}}^2 = \frac{\hat{V}_{\text{mod}}}{\hat{V}_{\text{Plas}}}. \quad (30)$$

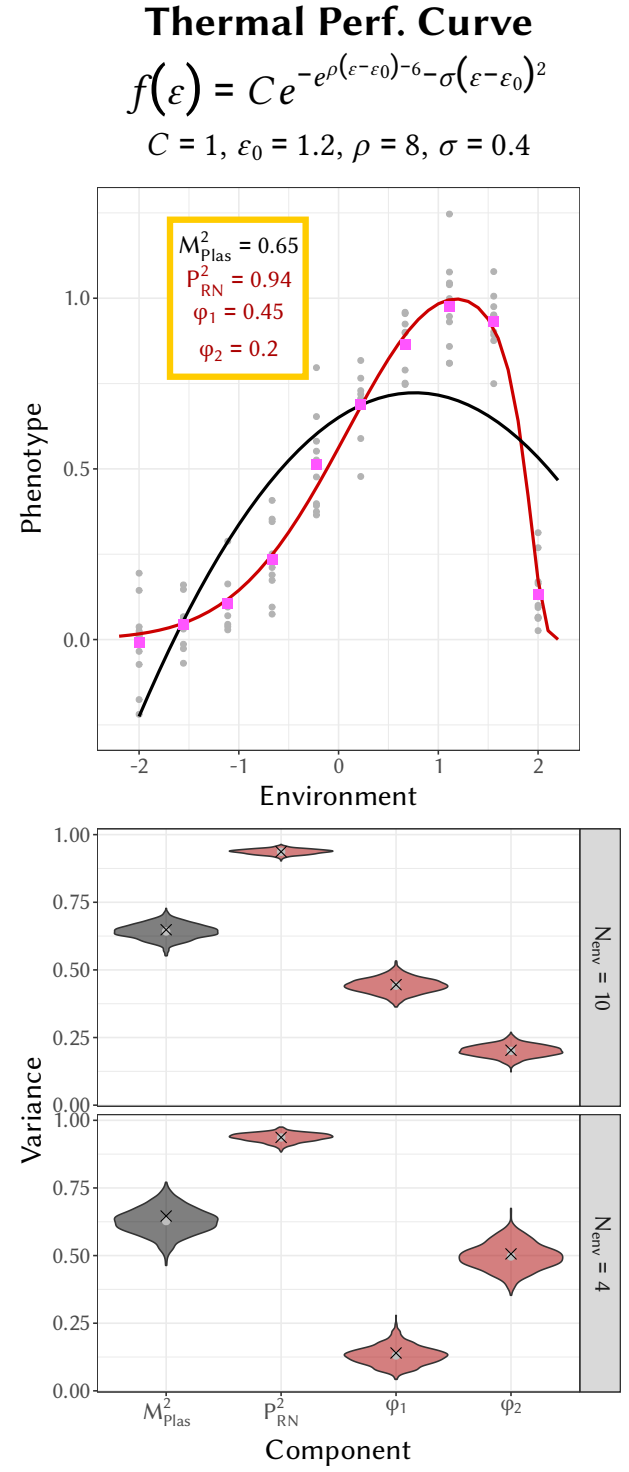
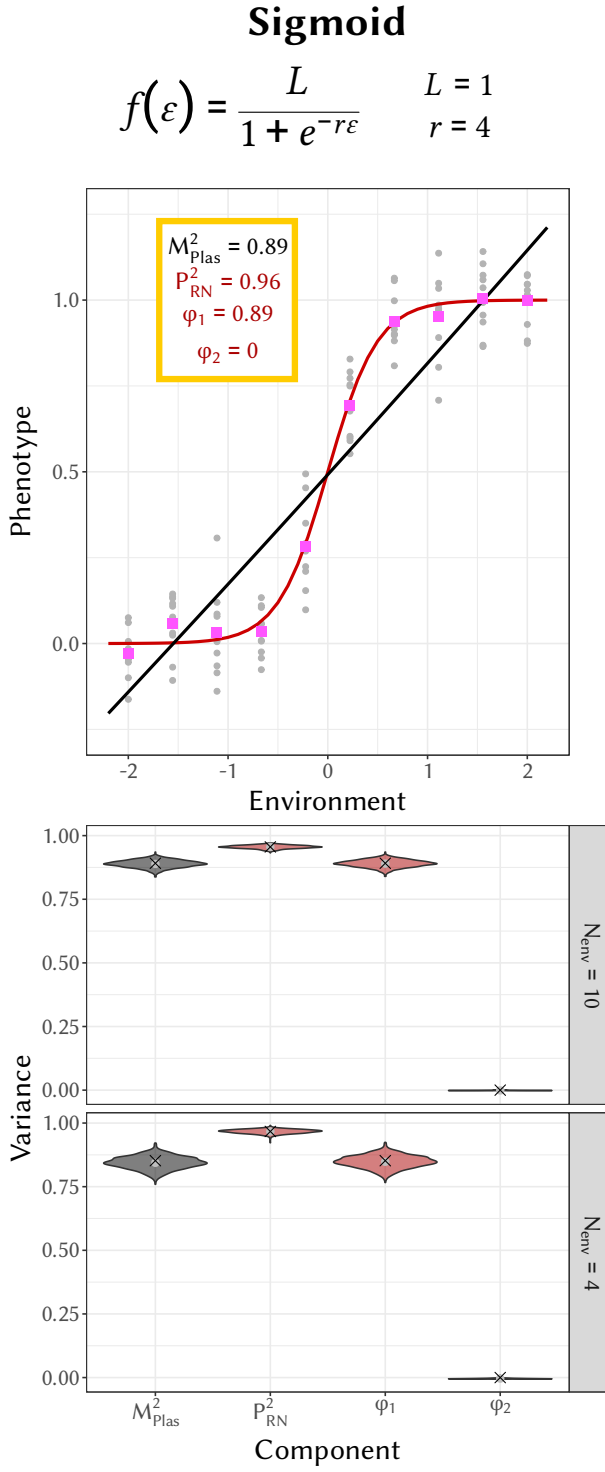


Figure 5: Estimation of the variance of the reaction norm when the true shape (sigmoid on the left, Gompertz-Gaussian performance curve on the right, red lines on top graphs) is unknown and approximated from a polynomial-Gaussian function. The estimated reaction norms using a polynomial function (black line, top graphs) only account for a part of the reaction norm shape, while the ANOVA estimation (pink dots, top graphs) fit the true shape more accurately. As a result, the model is expected to explain only a part M_{Plas}^2 of phenotypic variance due to plasticity. On the bottom rows, the error distribution are shown for M_{Plas}^2 , P_{RN}^2 , φ_1 and φ_2 (grey dots are the average estimated values, black crosses are the expected true values).

506 It is important to note here that M_{Plas}^2 is just a convenient way to quantify the amount of \hat{V}_{Plas}
 507 explained by the chosen parametric curve, and should not be used to perform model selection. Model

508 selection is a complex matter and we refer the readers to published reviews on this subject (e.g.
509 Johnson & Omland 2004; Tredennick et al. 2021).

510 In order to demonstrate the soundness and usefulness of this approach, we simulated datasets
511 following relatively common curves that are not well-captured by a second order polynomial: a logistic
512 sigmoid (hereafter sigmoid scenario), or a Gompertz-Gaussian thermal performance curve (hereafter
513 TPC scenario, see Figure 5). We assumed that the environment is sampled at either 10 or 4 values.
514 For each of these conditions, we simulated 1000 datasets, with 10 measures *per* environment (for
515 the sake of simplicity, and given the focus on \hat{P}_{RN}^2 here, we did not include different genotypes in
516 these simulations). We estimated the parameters of a polynomial model, and computed the relative
517 contributions of the first- and second-order parameters using Equation 16. In addition, we computed
518 the unbiased estimates of the variance explained by our polynomial or character-state models to obtain
519 M_{Plas}^2 .

520 Our results show that, as expected, the polynomial function is an imperfect proxy of our complex
521 shapes (Figure 5, $M_{Plas}^2 = 0.89$ for the sigmoid and $M_{Plas}^2 = 0.65$ for the TPC), but using the character-
522 state approach allows retrieving the total plastic variance without bias. The approach described here
523 is thus useful to compare a given reaction norm model (e.g. a polynomial function) to an unknown
524 true shape of the reaction norm, in a case where environment is discretised. In more detail, the linear
525 component was the most important component to explain the phenotypic variation for the sigmoid
526 scenario ($\varphi_1 = 0.89$, same as the total model). This was because the quadratic component was always
527 estimated close to zero ($< 10^{-3}$), thus no variance was explained by the quadratic component ($\varphi_2 = 0$).
528 Of course, the sigmoid is not a straight line either, and some remaining variance unexplained by the
529 polynomial curve ($1 - 0.89 = 0.11$) could have been explained by higher-order effects (e.g. cubic effect
530 and higher). By contrast, for the TPC scenario, while the linear component was an important factor
531 ($\varphi_1 = 0.47$), the quadratic component also explained quite a lot of the variance as well ($\varphi_2 = 0.2$).
532 Again, higher-order effect, including at least a cubic effect, would have explained more of the variance
533 arising from the average shape of plasticity.

534 This example illustrates the usefulness of a combined curve-parameter and character-state approach
535 to study the shape of reaction norms of a discretely sampled environment. While the character-
536 state approach provides a widely applicable estimation of \hat{P}_{RN}^2 (if the environment is discretised), the
537 curve-parameter approach provides interpretable information about (at least) first- and second-order
538 parameters of the reaction norm (although they might depart more or less strongly from its average
539 slope and curvature), which helps describing where most phenotypic variance lies. Our ratio M_{Plas}^2
540 can then be used to evaluate how well a chosen polynomial function models an actual reaction norm.

541 Estimation of non-linear models

542 Although we have focused so far on models that are linear in its parameters, the main strength of
543 our approach is its generality: it can be applied to any arbitrary functions (provided it is differen-
544 tiable). This requires numerically computing integrals for V_{Plas} (for \hat{P}_{RN}^2), π_{SI} , π_{CV} and ψ_ε (for the
545 heritabilities), but this can be solved with efficient algorithms. We illustrate this by introducing ge-
546 netic variation in the parameters of the sigmoid and TPC reaction norms illustrated in [Figure 5](#) (top
547 panels). We used a non-zero, but small, residual variance ($V_{\text{R}} = 0.0001$) to avoid numerical issues
548 typical when running thousands of non-linear models. We focused on a continuous environment, and
549 estimated the actual functions used to generate the datasets, using the non-linear modelling function
550 of nlme package (Pinheiro et al. 2009). We used the cubature package (Narasimhan et al. 2023), as
551 in the QGglimm package (de Villemereuil et al. 2016), to compute parameters linked to the variance
552 decomposition, and, further, the π -, γ - and ι -decomposition. We simulated 1000 datasets for each
553 scenario, consisting of 200 genotypes measured each in 10 different environments, randomly sampled
554 from a normal distribution.

555 We retrieved our simulated parameters without bias using the nlme function, except for a slight
556 bias (Wilcoxon’s rank test, $p < 0.05$) in the variance of r (latent slope) in the sigmoid model and
557 in C (height of the peak) in the TPC model. This translated into significant (Wilcoxon’s rank test,
558 $p < 0.05$), but very limited bias (relative bias $< 5\%$) in our derived parameters ([Figure 6](#), bottom
559 panels). Moreover, the sum of variance components (\hat{V}_{Tot}) successfully reflects the total phenotypic
560 variance, with a correlation between the two quantities $> 91\%$.

561 First focusing the average shape of the reaction norm ([Figure 6](#), top panel), one unfortunate aspect
562 of running a non-linear model is that our bias correction described in [Appendix E](#) can no longer be
563 applied. However, this bias is generally small provided the standard error is small for most parameters,
564 and the resulting bias in \hat{P}_{RN}^2 is extremely small, and even non-significant for the sigmoid model. An
565 important distinction here is the difference between the curve defined by the average parameters $f(\varepsilon, \bar{\theta})$
566 ([Figure 6](#), top panel, black curve) and the one defined by the local average phenotype $E_{g|\varepsilon}(\hat{z})$ ([Figure 6](#),
567 top panel, red curve), recalling that \hat{P}_{RN}^2 is linked to the latter. While the two are very close for the
568 sigmoid case, their differ quite visibly for the TPC one, due to a more pronounced non-linearity in the
569 parameters in the latter. The average slope contributed the most to the overall plastic variance of the
570 mean reaction norm for the sigmoid shape ($\pi_{\text{SI}} = 0.88$), with no impact of average curvature ($\pi_{\text{CV}} = 0$),
571 close to the φ -decomposition in [Figure 5](#). For the TPC scenario, the contribution of the average slope
572 ($\pi_{\text{SI}} = 0.31$) and curvature ($\pi_{\text{CV}} = 0.35$) are similar. In this case, the values are very different from

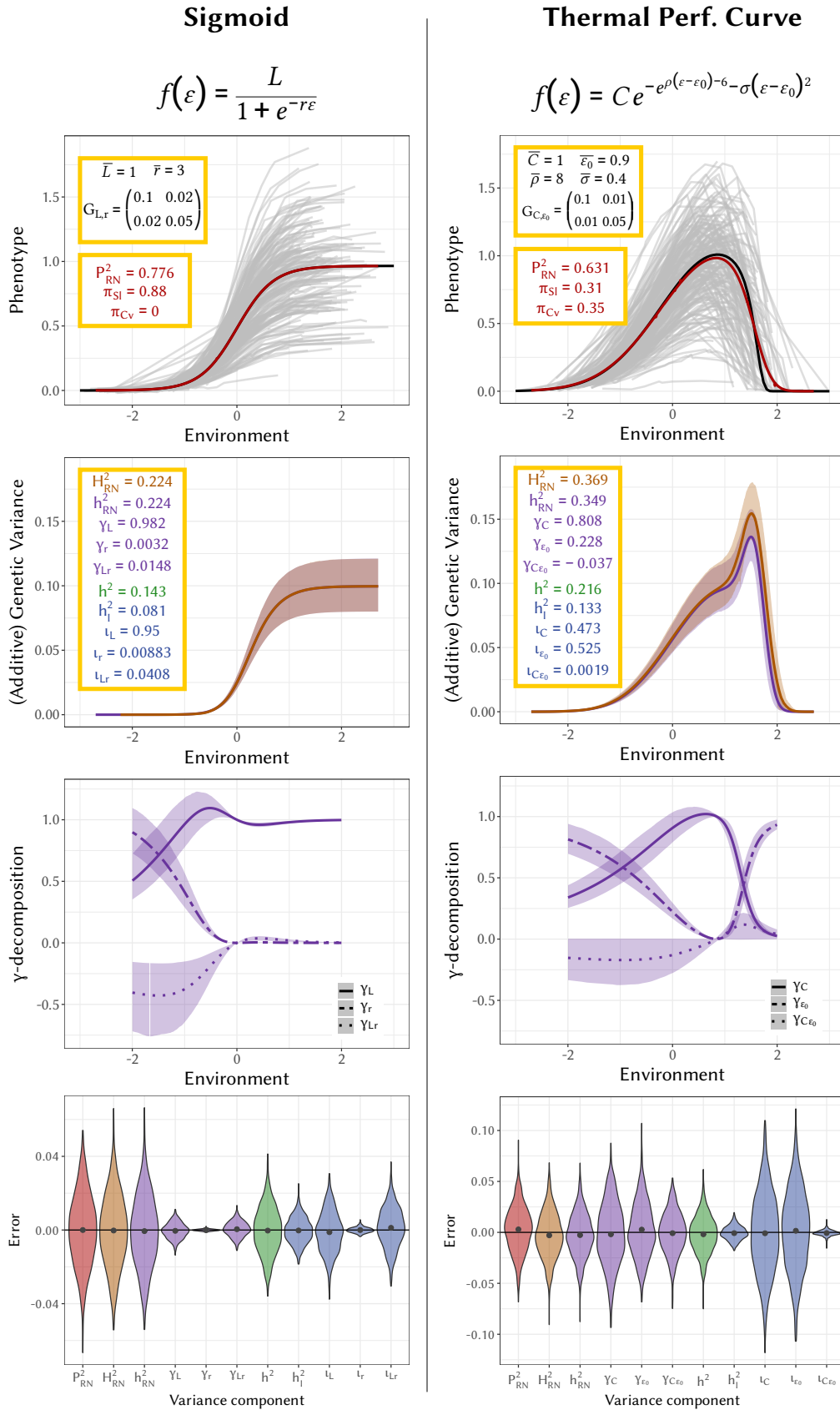


Figure 6: Scenarios and results of non-linear modelling of phenotypic plasticity in a continuous environment. On the left: results corresponding to a sigmoid curve scenario; on the right: results corresponding to a TPC scenario. First row: example of the individual curves (each curve corresponds to one individual) simulated in each scenario; yellow box: true parameters for the model and average shape; black curve : $f(\varepsilon, \hat{\theta})$; red curve : $E_{g|\varepsilon}(\hat{z})$. Second row: distribution of the estimations of $V_{G,\varepsilon}$ (brown) and $V_{A,\varepsilon}$ (purple), along the environment; solid line: average value across simulations; pale ribbon: 95% CI across simulations; yellow box: true values for the genetic variance partition. Third row: γ -decomposition of $V_{A,\varepsilon}$ along the environment, for each parameter and their covariation. Fourth row: distribution of the error for each component of our variance partition ("Variances") or for the π - and γ -decomposition ("Components"), red dot is the average of estimates over all simulations.

573 the φ -decomposition in Figure 5 (although note that the distribution of the environment is different
574 between these two scenarios). It might appear as counter-intuitive that the slope contributes so much
575 to variance, since the curve increases from 0 and then decreases toward 0, but this is linked to the fact
576 that the environment is normally distributed, so most values are near $\varepsilon = 0$, an area where the slope
577 of the curve is close to be maximised.

578 Although the variation between genotypes in the top panel of Figure 6 seems quite large, the
579 contribution from the average plasticity \hat{P}_{RN}^2 is 1.7 to 3.4 times higher than the one of the genetic
580 variance \hat{H}_{RN}^2 (Figure 6, yellow box in first- and second-row panels). This occurs because the genetic
581 variance is actually very low in most environments (Figure 6, brown and purple lines of the second-row
582 panels), and scarcely as high as V_{Plas} . As mentioned above, non-linearity in the parameters is less
583 strong for the sigmoid case than for the TPC case, resulting in almost exactly equal values for \hat{H}_{RN}^2
584 and \hat{h}_{RN}^2 for the former, while they are slightly different for the latter. In both cases, the low difference
585 between \hat{H}_{RN}^2 and \hat{h}_{RN}^2 can be explained by the disproportionate importance in the γ -decomposition of
586 parameters that are actually linearly related to the trait ($\gamma_L = 0.98$ for the sigmoid and $\gamma_C = 0.81$ for
587 the TPC scenarios). In terms of heritability of plasticity, it is substantial in both cases ($h_{\text{I}}^2 = 0.081$ for
588 the sigmoid and $h_{\text{I}}^2 = 0.133$ for the TPC scenario), as can be expected from the non-parallel reaction
589 norms (Figure 6). However, it remains smaller than the marginal heritability of the trait in both
590 cases ($h^2 = 0.143$ for the sigmoid and $h^2 = 0.216$ for the TPC scenarios). Interestingly, for the TPC
591 scenario, and contrary to what happens with the γ -decomposition, a majority of the additive genetic
592 variance in plasticity comes from the variation in the location of the optimum ($\iota_{\varepsilon_0} = 0.525$). This
593 is because variation in the location of the optimum shifts the reaction norm along the environment
594 axis (i.e. on the “x-axis”), meaning that even a small shift can generate considerable variation that is
595 non-parallel along the phenotype axis (i.e. along the “y-axis”).

596 An interesting aspect of our framework is that we can explore the variation of $V_{\text{Gen},\varepsilon}$, $V_{\text{A},\varepsilon}$ and
597 the γ -decomposition of $V_{\text{A},\varepsilon}$ along the environmental gradient, which can be very informative from
598 an evolutionary perspective. In the case of the sigmoid curve (Figure 6, second and third rows, left
599 panels), the analysis is relatively simple : as the value of the environment increases, the parameter L
600 is multiplied by an increased value (going from 0 to 1 due to the sigmoid function) and thus its genetic
601 variance plays a stronger role. This translates into $V_{\text{Gen},\varepsilon}$ and $V_{\text{A},\varepsilon}$ increasing with the environment,
602 and γ_L accounting for almost all of the genetic variance after the sigmoid inflexion point in 0. The
603 TPC scenario is even more interesting. First, we can see that both $V_{\text{Gen},\varepsilon}$ and $V_{\text{A},\varepsilon}$ (Figure 6, second
604 row, right panels) are close to zero in the extreme environments and maximised in a region between
605 the optimum and critical maximal temperature, where the reaction norm suddenly drops after the

606 optimum. This maximum also corresponds to the region where $V_{\text{Gen},\varepsilon}$ and $V_{\text{A},\varepsilon}$ are the most different
607 (and where the red and black departs the most in [Figure 6](#), top row, right panel). Regarding the
608 γ -decomposition ([Figure 6](#), third row, right panels), the influence of the location of the optimum (γ_{ε_0})
609 is maximised at extreme environments, while the influence of the maximum value at the peak (γ_C) is
610 exactly maximised at the average location of the peak. The influence of the covariation between both
611 ($\gamma_{C\varepsilon_0}$) is negative before the peak and positive after.

612 As these simulations illustrate, our framework allows very finely describing the characteristics of
613 reaction norms, such as how its average shape (slope/curvature) and genetic variation in the parameters
614 influence the phenotypic variance in the trait, while discriminating between total genetic variation of
615 the trait and genetic variation exclusively linked with plasticity itself.

616 Discussion

617 The variance decomposition in [Equation 7](#) is very general, and applicable to any approach used
618 to estimate a reaction norm. In particular, it applies equally well to both the character-state and
619 curve-parameter approaches. Each component and its variance-standardisation provide a different
620 information on the reaction norms: P_{RN}^2 quantifies the proportion of phenotypic variance due to the
621 average plastic response across genotypes, while H_{RN}^2 or h_{RN}^2 quantify the contributions from (broad or
622 additive) genetic variance in the reaction norms. Further, these genetic components can be separated
623 into the marginal heritability of the trait (h^2) based on the average breeding values across environments,
624 and the heritability of plasticity (h_{I}^2) which is solely based on the gene-by-environment interactions at
625 the level of breeding values. Finally, the sum $T_{\text{RN}}^2 = P_{\text{RN}}^2 + H_{\text{RN}}^2$ quantifies how well we can predict the
626 individual phenotypes based on their genotypes and environments (i.e. genetically variable reaction
627 norms). Those components are efficient summary statistics yielding important information regarding
628 the evolutionary potential of both the trait and its plasticity. Importantly, they are very generally
629 applicable, with a strict equivalence between e.g. a character-state or a curve-parameter approach.
630 However, they do not provide information regarding the actual shape of the reaction norms. To that
631 end, we further decomposed some of these components in terms of characteristics of the shape or
632 parameters of reaction norms.

633 The most difficult problem is to decompose the average plastic variance P_{RN}^2 into terms arising
634 either from the linear trend (π_{Sl}) or from the curvature (π_{Cv}) of the reaction norm, which we called
635 π -decomposition. Unfortunately, our estimates for π_{Sl} and π_{Cv} are only valid if the environment
636 is normally distributed, or the true reaction norm is quadratic. In other cases, mean slope and

637 curvature loose their simple interpretation, preventing a meaningful π -decomposition. Nonetheless,
638 for polynomial reaction norms of higher order, we described an alternative decomposition, based on
639 the polynomial coefficients rather than actual slope and curvature, which we called φ -decomposition.
640 While not as interpretable as the π -decomposition, this decomposition can serve as a way to com-
641 pare polynomial shapes across contexts. Based on the equivalence between the curve-parameter and
642 character-state, we introduced M_{Plas}^2 as a way to quantify the ability of a polynomial model to re-
643 cover V_{Plas} compared to an “agnostic” model such as the character-state. Our proposed framework is
644 summarised in [Figure 3](#).

645 Decomposing h_{RN}^2 and h_I^2 is comparatively easier, because the model assumed in [Equation 3](#)
646 and [Equation 4](#) ensures that we can always translate additive genetic variance in the parameters θ
647 into additive genetic variance in the trait z , even if the function f is not linear in its parameters.
648 Decomposition of the total heritability of the reaction norm h_{RN}^2 into the impact of the parameters
649 θ leads to the γ -decomposition. It quantifies the relative importance of genetic variance in different
650 reaction norm parameters to the evolvability of the trait. For instance if a given selection episode
651 concerns individuals that all experienced the same plasticity-inducing environment (i.e. when spatial
652 environmental variation is negligible relative to temporal variation), using the multivariate breeder’s
653 equation ([Lande 1979](#)), the relative contribution of genetic variation in parameter θ_i to the response
654 to selection for the trait z is

$$\frac{\Delta_{\theta_i} \bar{z}}{\Delta \bar{z}} = \gamma_i + \frac{1}{2} \sum_{i \neq j} \gamma_{ij}, \quad (31)$$

655 where the γ_i and γ_{ij} are defined in [Equation 26](#). In other words, the contributions of responses to
656 selection by different reaction norm parameters to overall response to selection by the plastic trait z
657 is directly proportional to their contribution to its genetic variance. Importantly, these contributions
658 will depend on the reaction norm gradient ψ_ε defined in [Equation 19](#), and thus on the environment,
659 as illustrated in [Equation 26](#). In fact, the environment-specific additive genetic variance $V_{A,\varepsilon}$ is a
660 critical piece of information regarding evolutionary potential, and we can apply the γ -decomposition
661 within each environment as well. For example, in the TPC scenario investigated above ([Figure 6](#), right
662 panels), the contribution of the peak height parameter C is maximised at the average location of the
663 optimum, where it accounts for 100% of the additive genetic variance. On the contrary, the influence of
664 additive genetic variation in the location of the optimum ε_0 is more important in extreme environments.
665 The complex interaction between the role of C and ε_0 generates a peak for $V_{A,\varepsilon}$ in the area between
666 the peak and critical maximal value for the environment (where the performance curve reaches zero).
667 In the context of predicting eco-evolutionary response to warming, this would mean that a slight
668 temperature rise above the optimum would provide a very short window of higher evolvability, but

669 followed by a sharp decrease thereof if warming persists. Beyond these simple scenarios, how selection
670 acts on reaction norms and plasticity depends on how the environment varies in space and/or time
671 (Scheiner 1993b; de Jong 1999; Tufto 2015; King & Hadfield 2019), and how the reaction norm gradient
672 ψ_ε and direction selection on the expressed trait z covary across environments. However, an in-depth
673 exploration of how to estimate these selection responses is beyond the scope of the present work.

674 While the γ -decomposition is key to understanding and predicting evolution of the trait, it is based
675 on the total heritability of the reaction norm h_{RN}^2 , which combines additive genetic variation in the
676 trait and its plasticity. To study plasticity in isolation from the marginal additive genetic variance in
677 the trait, we decomposed h_{I}^2 in a similar fashion as h_{RN}^2 , which we called the ι -decomposition. The
678 components of the ι -decomposition measure the contribution of each parameter to the evolutionary
679 potential of plasticity, i.e. to the evolvability of reaction norm shape. In our thermal performance case
680 (TPC) example, the ι associated to C and ε_0 were close to 0.5, meaning that evolution can roughly
681 equally impact the peak height C or the location of the optimum ε_0 , should selection on the shape of
682 reaction norms occur.

683 The detailed decomposition that we propose open the door to better commensurability and com-
684 parability across studies, which can be a challenge in meta-analyses of plasticity. Murren et al. (2014)
685 performed such a meta-analysis, comparing genetic variation in different parameters of reaction norm
686 shape across published datasets. However they (i) computed these parameters using only extreme
687 environmental values, instead of the whole range of environments; (ii) did not account for uneven
688 spacing between environments where relevant; (iii) did not account for uncertainty in estimations
689 of reaction norms (as previously highlighted by Morrissey & Liefting 2016); and (iv) assumed the
690 modeled reaction norm shape is true. More detail about the analyses in that study is provided in
691 [Appendix G](#). Our approach overcomes all these issues (some of which had been dealt with already
692 by Morrissey & Liefting 2016). Unfortunately the dataset compiled by Murren et al. (2014) does
693 not provide information on uncertainty of phenotypic estimates (related to V_{Res}), precluding proper
694 meta-analysis of reaction norm shape variation.

695 Importantly, our variance partitioning can be implemented through commonly used statistical
696 models, notably (non-)linear mixed models. We showed that even complex non-linear modelling can
697 perform well, only at the cost of using dedicated libraries to compute integrals numerically. This
698 means that biologists can readily seize all the modelling tools introduced here. In particular, although
699 a character-state approach can be performed using a simple random-intercept model, studies of genetic
700 variance in plasticity seem to rather use a multi-trait model, which offers more control, but is more diffi-
701 cult to implement (but see Stirling & Roff 2000). In order to make the variance partitioning introduced

702 here more accessible, we have implemented the computation of \hat{P}_{RN}^2 and the heritabilities, as well as
703 their different decompositions as an R package named Reacnorm github.com/devillemereuil/Reacnorm.
704 The package also included a tutorial as a vignette, showing how to implement the models in the
705 Bayesian package brms and use functions from Reacnorm to study the properties of reaction norms.
706 We hope that this will further stimulate interest in investigating variation and evolutionary potential
707 of reaction norms.

708 **Code availability** The code for the data simulation and analyses performed in this article is available
709 at the following repository: github.com/devillemereuil/CodePartReacnorm

710 **Acknowledgements** We are grateful to Jarrod Hadfield, Thibaut Morel-Journel, Stéphane Robin
711 and John Stinchcombe for useful discussions and/or comments that much improved the quality of the
712 paper.

713 References

- 714 Albecker, M. A., Trussell, G. C., & Lotterhos, K. E. (2022) A novel analytical framework to quantify
715 co-gradient and countergradient variation. *Ecology Letters*, 25:(2022), 1521–1533. doi: [10.1111/ele.](https://doi.org/10.1111/ele.14020)
716 [14020](https://doi.org/10.1111/ele.14020).
- 717 Angilletta, M. J. (2009) *Thermal adaptation: a theoretical and empirical synthesis*. OUP Oxford,
718 Jan. 29, 2009. 304 pp.
- 719 Bates, D., Mächler, M., Bolker, B., & Walker, S. (2015) Fitting linear mixed-effects models using lme4.
720 *Journal of Statistical Software*, 67:(2015), 48.
- 721 Bonamour, S., Chevin, L.-M., Charmantier, A., & Teplitsky, C. (2019) Phenotypic plasticity in re-
722 sponse to climate change: the importance of cue variation. *Philosophical Transactions of the Royal*
723 *Society B: Biological Sciences*, 374:(Mar. 18, 2019), 20180178. doi: [10.1098/rstb.2018.0178](https://doi.org/10.1098/rstb.2018.0178).
- 724 Bradshaw, A. D. (1965) Evolutionary significance of phenotypic plasticity in plants. *Advances in*
725 *Genetics*. Ed. by E. W. Caspari & J. M. Thoday. Vol. 13. Cambridge (MA, USA): Academic Press,
726 Jan. 1, 1965, pp. 115–155. doi: [10.1016/S0065-2660\(08\)60048-6](https://doi.org/10.1016/S0065-2660(08)60048-6).
- 727 Brown, G. G. & Rutenmiller, H. C. (1977) Means and variances of stochastic vector products with
728 applications to random linear models. *Management Science*, 24:(Oct. 1977), 210–216. doi: [10.](https://doi.org/10.1287/mnsc.24.2.210)
729 [1287/mnsc.24.2.210](https://doi.org/10.1287/mnsc.24.2.210).
- 730 Bürkner, P.-C. (2017) Advanced bayesian multilevel modeling with the R package brms. *ArXiv170511123*
731 *Stat:*(May 31, 2017).

- 732 Charmantier, A., McCleery, R. H., Cole, L. R., Perrins, C., Kruuk, L. E. B., & Sheldon, B. C. (2008)
733 Adaptive phenotypic plasticity in response to climate change in a wild bird population. *Science*,
734 320:(May 9, 2008), 800–803. doi: [10.1126/science.1157174](https://doi.org/10.1126/science.1157174).
- 735 Chevin, L.-M., Collins, S., & Lefèvre, F. (2013) Phenotypic plasticity and evolutionary demographic
736 responses to climate change: taking theory out to the field. *Functional Ecology*, 27:(2013), 967–979.
737 doi: [10.1111/j.1365-2435.2012.02043.x](https://doi.org/10.1111/j.1365-2435.2012.02043.x).
- 738 Chevin, L.-M., Lande, R., & Mace, G. M. (2010) Adaptation, plasticity, and extinction in a changing
739 environment: towards a predictive theory. *PLOS Biology*, 8:(Apr. 27, 2010), e1000357. doi: [10.1371/
740 journal.pbio.1000357](https://doi.org/10.1371/journal.pbio.1000357).
- 741 de Jong, G. (1990) Quantitative genetics of reaction norms. *Journal of evolutionary biology*, 3:(1990),
742 447–468.
- 743 de Jong, G. (1995) Phenotypic plasticity as a product of selection in a variable environment. *The*
744 *American Naturalist*, 145:(Apr. 1, 1995), 493–512. doi: [10.1086/285752](https://doi.org/10.1086/285752).
- 745 de Jong, G. (1999) Unpredictable selection in a structured population leads to local genetic differen-
746 tiation in evolved reaction norms. *Journal of Evolutionary Biology*, 12:(1999), 839–851.
- 747 Des Marais, D. L., Hernandez, K. M., & Juenger, T. E. (2013) Genotype-by-environment interaction
748 and plasticity: exploring genomic responses of plants to the abiotic environment. *Annual Review of*
749 *Ecology, Evolution, and Systematics*, 44:(2013), 5–29. doi: [10.1146/annurev-ecolsys-110512-135806](https://doi.org/10.1146/annurev-ecolsys-110512-135806).
- 750 Deutsch, C. A., Tewksbury, J. J., Huey, R. B., Sheldon, K. S., Ghalambor, C. K., Haak, D. C., & Martin,
751 P. R. (2008) Impacts of climate warming on terrestrial ectotherms across latitude. *Proceedings of*
752 *the National Academy of Sciences*, 105:(May 6, 2008), 6668–6672. doi: [10.1073/pnas.0709472105](https://doi.org/10.1073/pnas.0709472105).
- 753 de Villemereuil, P. (2018) Quantitative genetic methods depending on the nature of the phenotypic
754 trait. *Annals of the New York Academy of Sciences*. The Year in Evolutionary Biology 1422:(June 1,
755 2018), 29–47. doi: [10.1111/nyas.13571](https://doi.org/10.1111/nyas.13571).
- 756 de Villemereuil, P., Morrissey, M. B., Nakagawa, S., & Schielzeth, H. (2018) Fixed-effect variance and
757 the estimation of repeatabilities and heritabilities: issues and solutions. *Journal of Evolutionary*
758 *Biology*, 31:(2018), 621–632. doi: [10.1111/jeb.13232](https://doi.org/10.1111/jeb.13232).
- 759 de Villemereuil, P., Schielzeth, H., Nakagawa, S., & Morrissey, M. B. (2016) General methods for
760 evolutionary quantitative genetic inference from generalised mixed models. *Genetics*, 204:(Nov. 1,
761 2016), 1281–1294. doi: [10.1534/genetics.115.186536](https://doi.org/10.1534/genetics.115.186536).
- 762 de Villemereuil, P. et al. (2020) Fluctuating optimum and temporally variable selection on breeding
763 date in birds and mammals. *Proceedings of the National Academy of Sciences*, 117:(2020), 31969–
764 31978. doi: [10.1073/pnas.2009003117](https://doi.org/10.1073/pnas.2009003117).

- 765 Falconer, D. S. (1952) The problem of environment and selection. *The American Naturalist*, 86:(Sept. 1,
766 1952), 293–298. doi: [10.1086/281736](https://doi.org/10.1086/281736).
- 767 Falconer, D. S. & Mackay, T. F. (1996) *Introduction to quantitative genetics*. 4th ed. Harlow, Essex
768 (UK): Benjamin Cummings, Feb. 16, 1996.
- 769 Gavrillets, S. & Scheiner, S. M. (1993a) The genetics of phenotypic plasticity. V. Evolution of reaction
770 norm shape. *Journal of Evolutionary Biology*, 6:(1993), 31–48. doi: [10.1046/j.1420-9101.1993.
771 6010031.x](https://doi.org/10.1046/j.1420-9101.1993.6010031.x).
- 772 Gavrillets, S. & Scheiner, S. M. (1993b) The genetics of phenotypic plasticity. VI. Theoretical predic-
773 tions for directional selection. *Journal of Evolutionary Biology*, 6:(1993), 49–68.
- 774 Gienapp, P., Teplitsky, C., Alho, J. S., Mills, J. A., & Merilä, J. (2008) Climate change and evolution:
775 disentangling environmental and genetic responses. *Molecular Ecology*, 17:(Jan. 1, 2008), 167–178.
776 doi: [10.1111/j.1365-294X.2007.03413.x](https://doi.org/10.1111/j.1365-294X.2007.03413.x).
- 777 Gomulkiewicz, R. & Kirkpatrick, M. (1992) Quantitative genetics and the evolution of reaction norms.
778 *Evolution*, 46:(Apr. 1, 1992), 390–411. doi: [10.1111/j.1558-5646.1992.tb02047.x](https://doi.org/10.1111/j.1558-5646.1992.tb02047.x).
- 779 Hammill, E., Rogers, A., & Beckerman, A. P. (2008) Costs, benefits and the evolution of inducible
780 defences: a case study with *Daphnia pulex*. *Journal of Evolutionary Biology*, 21:(May 1, 2008),
781 705–715. doi: [10.1111/j.1420-9101.2008.01520.x](https://doi.org/10.1111/j.1420-9101.2008.01520.x).
- 782 Johnson, J. B. & Omland, K. S. (2004) Model selection in ecology and evolution. *Trends in Ecology*
783 *& Evolution*, 19:(Feb. 2004), 101–108. doi: [doi:DOI:10.1016/j.tree.2003.10.013](https://doi.org/10.1016/j.tree.2003.10.013).
- 784 Johnson, P. C. (2014) Extension of Nakagawa & Schielzeth’s R2GLMM to random slopes models.
785 *Methods in Ecology and Evolution*, 5:(Sept. 1, 2014), 944–946. doi: [10.1111/2041-210X.12225](https://doi.org/10.1111/2041-210X.12225).
- 786 King, J. G. & Hadfield, J. D. (2019) The evolution of phenotypic plasticity when environments fluctuate
787 in time and space. *Evolution Letters*, 3:(Feb. 1, 2019), 15–27. doi: [10.1002/evl3.100](https://doi.org/10.1002/evl3.100).
- 788 Kirkpatrick, M. (2009) Patterns of quantitative genetic variation in multiple dimensions. *Genetica*,
789 136:(June 1, 2009), 271–284. doi: [10.1007/s10709-008-9302-6](https://doi.org/10.1007/s10709-008-9302-6).
- 790 Kirkpatrick, M. & Heckman, N. (1989) A quantitative genetic model for growth, shape, reaction norms,
791 and other infinite-dimensional characters. *Journal of Mathematical Biology*, 27:(Aug. 1, 1989), 429–
792 450. doi: [10.1007/BF00290638](https://doi.org/10.1007/BF00290638).
- 793 Lande, R. (1979) Quantitative genetic analysis of multivariate evolution, applied to brain:body size
794 allometry. *Evolution*, 33:(1979), 402–416.
- 795 Lande, R. (2009) Adaptation to an extraordinary environment by evolution of phenotypic plasticity
796 and genetic assimilation. *Journal of Evolutionary Biology*, 22:(July 1, 2009), 1435–1446. doi: [10.
797 1111/j.1420-9101.2009.01754.x](https://doi.org/10.1111/j.1420-9101.2009.01754.x).

- 798 Lande, R. & Arnold, S. J. (1983) The measurement of selection on correlated characters. *Evolution*,
799 37:(1983), 1210–1226. doi: [10.2307/2408842](https://doi.org/10.2307/2408842).
- 800 Landsman, Z. & Nešlehová, J. (2008) Stein’s Lemma for elliptical random vectors. *Journal of Multi-*
801 *variate Analysis*, 99:(May 1, 2008), 912–927. doi: [10.1016/j.jmva.2007.05.006](https://doi.org/10.1016/j.jmva.2007.05.006).
- 802 Landsman, Z., Vanduffel, S., & Yao, J. (2013) A note on Stein’s lemma for multivariate elliptical
803 distributions. *Journal of Statistical Planning and Inference*, 143:(Nov. 1, 2013), 2016–2022. doi:
804 [10.1016/j.jspi.2013.06.003](https://doi.org/10.1016/j.jspi.2013.06.003).
- 805 Lynch, M. & Walsh, B. (1998) *Genetics and analysis of quantitative traits*. Sunderland, Massachussets
806 (US): Sinauer Associates, 1998.
- 807 Lynch, M. & Gabriel, W. (1987) Environmental tolerance. *The American Naturalist*, 129:(Feb. 1, 1987),
808 283–303. doi: [10.1086/284635](https://doi.org/10.1086/284635).
- 809 Merilä, J. & Hendry, A. P. (2014) Climate change, adaptation, and phenotypic plasticity: the problem
810 and the evidence. *Evolutionary Applications*, 7:(2014), 1–14. doi: [10.1111/eva.12137](https://doi.org/10.1111/eva.12137).
- 811 Mitchell, D. J. & Houslay, T. M. (2021) Context-dependent trait covariances: how plasticity shapes
812 behavioral syndromes. *Behavioral Ecology*, 32:(Jan. 1, 2021), 25–29. doi: [10.1093/beheco/araa115](https://doi.org/10.1093/beheco/araa115).
- 813 Moczek & Emlen (1999) Proximate determination of male horn dimorphism in the beetle *Onthophagus*
814 *taurus* (Coleoptera: Scarabaeidae). *Journal of Evolutionary Biology*, 12:(1999), 27–37. doi: [10.1046/
815 j.1420-9101.1999.00004.x](https://doi.org/10.1046/j.1420-9101.1999.00004.x).
- 816 Morrissey, M. B. (2015) Evolutionary quantitative genetics of nonlinear developmental systems. *Evo-*
817 *lution*, 69:(Aug. 1, 2015), 2050–2066. doi: [10.1111/evo.12728](https://doi.org/10.1111/evo.12728).
- 818 Morrissey, M. B. & Liefting, M. (2016) Variation in reaction norms: Statistical considerations and
819 biological interpretation. *Evolution*, 70:(Sept. 1, 2016), 1944–1959. doi: [10.1111/evo.13003](https://doi.org/10.1111/evo.13003).
- 820 Murren, C. J., Maclean, H. J., Diamond, S. E., Steiner, U. K., Heskell, M. A., Handelsman, C. A.,
821 Ghalambor, C. K., Auld, J. R., Callahan, H. S., & Pfennig, D. W. (2014) Evolutionary change in
822 continuous reaction norms. *The American Naturalist*, 183:(2014), 453–467.
- 823 Nakagawa, S. & Schielzeth, H. (2013) A general and simple method for obtaining R² from generalized
824 linear mixed-effects models. *Methods in Ecology and Evolution*, 4:(2013), 133–142. doi: [10.1111/j.
825 2041-210x.2012.00261.x](https://doi.org/10.1111/j.2041-210x.2012.00261.x).
- 826 Narasimhan, B., Johnson, S. G., Hahn, T., Bouvier, A., & Kiêu, K. (2023) *Cubature: Adaptive multi-*
827 *variate integration over hypercubes*. manual. 2023.
- 828 Nussey, D. H., Postma, E., Gienapp, P., & Visser, M. E. (2005) Selection on heritable phenotypic
829 plasticity in a wild bird population. *Science*, 310:(Oct. 14, 2005), 304–306. doi: [10.1126/science.
830 1117004](https://doi.org/10.1126/science.1117004).

- 831 Pinheiro, J., Bates, D., DebRoy, S., Sarkar, D., & {the R Core team} (2009) *Nlme: Linear and*
832 *Nonlinear Mixed Effects Models*. 2009.
- 833 Pletcher, S. D. & Geyer, C. J. (1999) The genetic analysis of age-dependent traits: modeling the
834 character process. *Genetics*, 153:(Oct. 1, 1999), 825–835. doi: [10.1093/genetics/153.2.825](https://doi.org/10.1093/genetics/153.2.825).
- 835 Reed, T. E., Waples, R. S., Schindler, D. E., Hard, J. J., & Kinnison, M. T. (2010) Phenotypic plasticity
836 and population viability: the importance of environmental predictability. *Proceedings of the Royal*
837 *Society B: Biological Sciences*, 277:(Nov. 22, 2010), 3391–3400. doi: [10.1098/rspb.2010.0771](https://doi.org/10.1098/rspb.2010.0771).
- 838 Rice, S. H. (2004) *Evolutionary Theory: Mathematical and Conceptual Foundations*. Sinauer, Sept. 1,
839 2004. 348 pp.
- 840 Robertson, A. (1966) A mathematical model of the culling process in dairy cattle. *Animal Science*,
841 8:(1966), 95–108. doi: [10.1017/S0003356100037752](https://doi.org/10.1017/S0003356100037752).
- 842 Rovelli, G. et al. (2020) The genetics of phenotypic plasticity in livestock in the era of climate change:
843 a review. *Italian Journal of Animal Science*, 19:(Dec. 14, 2020), 997–1014. doi: [10.1080/1828051X.](https://doi.org/10.1080/1828051X.2020.1809540)
844 [2020.1809540](https://doi.org/10.1080/1828051X.2020.1809540).
- 845 Schaum, C. E. & Collins, S. (2014) Plasticity predicts evolution in a marine alga. *Proceedings of the*
846 *Royal Society B: Biological Sciences*, 281:(Oct. 22, 2014), 20141486. doi: [10.1098/rspb.2014.1486](https://doi.org/10.1098/rspb.2014.1486).
- 847 Scheiner, S. M. (1993a) Genetics and evolution of phenotypic plasticity. *Annual Review of Ecology and*
848 *Systematics*, 24:(Nov. 1993), 35–68. doi: [10.1146/annurev.es.24.110193.000343](https://doi.org/10.1146/annurev.es.24.110193.000343).
- 849 Scheiner, S. M. (1993b) Plasticity as a selectable trait: reply to Via. *The American Naturalist*, 142:(Aug. 1,
850 1993), 371–373. doi: [10.1086/285544](https://doi.org/10.1086/285544).
- 851 Scheiner, S. M. & Lyman, R. F. (1989) The genetics of phenotypic plasticity I. Heritability. *Journal*
852 *of Evolutionary Biology*, 2:(Mar. 1989), 95–107. doi: [10.1046/j.1420-9101.1989.2020095.x](https://doi.org/10.1046/j.1420-9101.1989.2020095.x).
- 853 Schlichting, C. D. & Pigliucci, M. (1998) Phenotypic evolution: a reaction norm perspective. *Pheno-*
854 *typic evolution: a reaction norm perspective.*:(1998).
- 855 Stinchcombe, J. R., Function-valued Traits Working Group, & Kirkpatrick, M. (2012) Genetics and
856 evolution of function-valued traits: understanding environmentally responsive phenotypes. *Trends*
857 *in Ecology & Evolution*, 27:(Nov. 1, 2012), 637–647. doi: [10.1016/j.tree.2012.07.002](https://doi.org/10.1016/j.tree.2012.07.002).
- 858 Stirling, G. & Roff, D. A. (2000) Behaviour plasticity without learning: phenotypic and genetic vari-
859 ation of naïve *Daphnia* in an ecological trade-off. *Animal Behaviour*, 59:(May 1, 2000), 929–941.
860 doi: [10.1006/anbe.1999.1386](https://doi.org/10.1006/anbe.1999.1386).
- 861 Suzuki, Y. & Nijhout, H. F. (2006) Evolution of a polyphenism by genetic accommodation. *Science*,
862 311:(Feb. 3, 2006), 650–652. doi: [10.1126/science.1118888](https://doi.org/10.1126/science.1118888).

- 863 Teplitsky, C., Mills, J. A., Alho, J. S., Yarrall, J. W., & Merilä, J. (2008) Bergmann's rule and climate
864 change revisited: Disentangling environmental and genetic responses in a wild bird population.
865 *Proceedings of the National Academy of Sciences*, 105:(Sept. 9, 2008), 13492–13496. doi: [10.1073/
866 pnas.0800999105](https://doi.org/10.1073/pnas.0800999105).
- 867 Tredennick, A. T., Hooker, G., Ellner, S. P., & Adler, P. B. (2021) A practical guide to selecting
868 models for exploration, inference, and prediction in ecology. *Ecology*, 102:(2021), e03336. doi: [10.
869 1002/ecy.3336](https://doi.org/10.1002/ecy.3336).
- 870 Tufto, J. (2000) The evolution of plasticity and nonplastic spatial and temporal adaptations in the
871 presence of imperfect environmental cues. *The American Naturalist*, 156:(Aug. 1, 2000), 121–130.
872 doi: [10.1086/303381](https://doi.org/10.1086/303381).
- 873 Tufto, J. (2015) Genetic evolution, plasticity, and bet-hedging as adaptive responses to temporally
874 autocorrelated fluctuating selection: A quantitative genetic model. *Evolution*, 69:(2015), 2034–
875 2049. doi: [10.1111/evo.12716](https://doi.org/10.1111/evo.12716).
- 876 Vedder, O., Bouwhuis, S., & Sheldon, B. C. (2013) Quantitative assessment of the importance of
877 phenotypic plasticity in adaptation to climate change in wild bird populations. *PLOS Biology*,
878 11:(2013), e1001605. doi: [10.1371/journal.pbio.1001605](https://doi.org/10.1371/journal.pbio.1001605).
- 879 Via, S. & Lande, R. (1985) Genotype-environment interaction and the evolution of phenotypic plas-
880 ticity. *Evolution*, 39:(May 1, 1985), 505–522. doi: [10.1111/j.1558-5646.1985.tb00391.x](https://doi.org/10.1111/j.1558-5646.1985.tb00391.x).
- 881 Wilson, A. J., Réale, D., Clements, M. N., Morrissey, M. M., Postma, E., Walling, C. A., Kruuk,
882 L. E. B., & Nussey, D. H. (2010) An ecologist's guide to the animal model. *Journal of Animal
883 Ecology*, 79:(Jan. 2010), 13–26. doi: [10.1111/j.1365-2656.2009.01639.x](https://doi.org/10.1111/j.1365-2656.2009.01639.x).
- 884 Woltereck, R. (1909) Weitere experimentelle Untersuchungen über Artveränderung, speziell über das
885 Wesen quantitativer Artunterschiede bei Daphniden. *Verh. D. Tsch. Zool. Ges.*, 1909:(1909), 110–
886 172.

Appendix

887

888 **A A unified formalism for the curve-parameters and** 889 **character-state approaches**

890 Despite having different mechanics, the curve-parameter and character-state approaches can be shown
891 to be mathematically equivalent de Jong (1995). We can use this to express both approaches under
892 the same, unified formalism. More precisely, we can express the character-state approach as being
893 a special case of the curve-parameters approach. Under a curve-parameters approach, the reaction
894 norm is seen as a function f of the environment ε and a vector of parameters $\boldsymbol{\theta}_g$:

$$\hat{z} = f(\varepsilon, \boldsymbol{\theta}_g). \quad (\text{S1})$$

895 The $\boldsymbol{\theta}_g$'s covary across genotypes with a variance-covariance matrix \mathbf{G}_θ :

$$\boldsymbol{\theta}_g \sim \mathcal{N}(\bar{\boldsymbol{\theta}}, \mathbf{G}_\theta). \quad (\text{S2})$$

896 By contrast, in a character-state approach, the reaction norm values of different genotypes across
897 environments are directly provided by sampling from a multivariate normal distribution:

$$\hat{z} \sim \mathcal{N}(\boldsymbol{\mu}, \mathbf{G}_z). \quad (\text{S3})$$

898 One way to express the character-state using the same formalism as the curve-parameter is to recognise
899 that Equation S3 can be written as

$$\begin{aligned} \hat{z} &= \boldsymbol{\mu}_g^T \mathbf{u}_k, \\ \boldsymbol{\mu}_g &\sim \mathcal{N}(\boldsymbol{\mu}, \mathbf{G}_z), \end{aligned} \quad (\text{S4})$$

900 where \mathbf{u}_k is the unit vector with 1 at the k th value (corresponding to environment ε_k) and 0 elsewhere.
901 Thus, the character-state model can be expressed using the formalism of Equation S1 and Equation S2,
902 where $\boldsymbol{\mu}_g$ in Equation S4 plays the role of $\boldsymbol{\theta}_g$, and thus \mathbf{G}_z plays the role of \mathbf{G}_θ . In this case, the
903 function f is a function taking the level k of the environment and the parameters $\boldsymbol{\mu}_g$ of the genotype
904 g as input, and yielding the evaluated reaction norm \hat{z} as the output. Evidently, this function f is
905 not continuous and not differentiable along the (categorical) environment. However, it is a continuous,
906 differentiable and even linear function along the (continuous) parameters $\boldsymbol{\mu}_g$. As such, all properties
907 mentioned in the main text and the Appendices pertaining to reaction norms that are “linear in its

908 parameters” also apply to the character-state approach.

909 **B Computation of the additive genetic variance holding** 910 **environment constant**

911 **B1 Preliminary results**

912 **Multiple regression slopes expressed using a variance-covariance matrix** Let us assume a multiple
913 regression between a random variable y and a set of random variables $\mathbf{x} = (x_1, \dots, x_n)^T$ such that:

$$y = \mu + \mathbf{x}^T \boldsymbol{\beta} + e, \quad (\text{S5})$$

914 where μ is the intercept and e is the residual of the model. Note that in practical regression, the realised
915 sampling of \mathbf{x} will be contained in the design matrix of the model. If it exists and is unique, the solution
916 for the vector of multiple regression slopes $\boldsymbol{\beta}$ can be formulated in terms variance-covariance matrices
917 (see e.g. p.179, Lynch & Walsh 1998):

$$\boldsymbol{\beta} = \mathbf{V}(\mathbf{x})^{-1} \text{cov}(\mathbf{x}, y), \quad (\text{S6})$$

918 where $\mathbf{V}(\mathbf{x})$ is the variance-covariance matrix of \mathbf{x} , $\mathbf{V}(\mathbf{x})^{-1}$ is its inverse matrix and $\text{cov}(\mathbf{x}, y)$ is the
919 column-vector of covariances between the x_i and y .

920 **Multivariate version of Stein’s lemma** Let us assume that $\mathbf{x} = (x_1, \dots, x_{p_x})$ and $\mathbf{y} = (y_1, \dots, y_{p_y})$
921 follow multivariate normal distributions, and that g is a differentiable, $R^{p_x} \rightarrow R$ function such that
922 $\text{E}(\nabla g)$, where ∇g is the gradient of g (the vector of partial derivatives), is a vector with finite values,
923 then it can be shown (Landsman & Nešlehová 2008; Landsman et al. 2013) that:

$$\text{cov}(g(\mathbf{x}), \mathbf{y}) = \text{cov}(\mathbf{x}, \mathbf{y}) \text{E}(\nabla g). \quad (\text{S7})$$

924 Note that covariance matrices of vectors (also known as cross-covariance matrices) are not commuta-
925 tive, but are such that $\text{cov}(\mathbf{x}, \mathbf{y}) = \text{cov}(\mathbf{y}, \mathbf{x})^T$. In the case where $p_y = 1$, then $\mathbf{y} = y$ follows a normal
926 distribution and:

$$\text{cov}(g(\mathbf{x}), y) = \text{cov}(y, \mathbf{x}) \text{E}(\nabla g). \quad (\text{S8})$$

927 Note that $\text{cov}(y, \mathbf{x})$ is a row-vector and $\text{cov}(\mathbf{x}, y)$ is a column-vector by convention.

928 **B2 Breeding values in a given environment**

929 **Genetics of reaction norms** As mentioned in the main text, a general formalism (including the
930 character-state as a special case) for the reaction norm \hat{z} is given by [Equation 3](#) in the main text, i.e.

$$\hat{z} = f(\varepsilon, \boldsymbol{\theta}_g). \quad (\text{S9})$$

931 The phenotype predicted by the reaction norm \hat{z} thus depends on the environmental value ε , and the
932 reaction norm parameters $\boldsymbol{\theta}_g$ specific to the genotype g . When holding the environment ε constant,
933 the genetic variance is simply the variance of reaction norms across genotypes:

$$V_{G|\varepsilon} = V_{g|\varepsilon}(f(\varepsilon, \boldsymbol{\theta}_g)) \quad (\text{S10})$$

934 If the reaction norms are estimated in such a way that non-additive genetic variance can be separated
935 out from additive genetic variance (e.g. if “genotype” refers to individuals) or are known to be negligible
936 on the one hand; and if the reaction norm is linear in its parameters (i.e. f is a linear function of $\boldsymbol{\theta}_g$,
937 as for a polynomial function) on the other hand, then the additive genetic variance conditional on the
938 environment is readily given by [Equation S10](#), i.e. $V_{A|\varepsilon} = V_{G|\varepsilon}$. In the case where f is not linear in its
939 parameters, it is necessary to rely on the theory in non-linear quantitative genetics ([Morrissey 2015](#);
940 [de Villemereuil et al. 2016](#)), as we do below.

941 **Linear relationship between breeding values** The relationship between the breeding value of the
942 trait \mathcal{A}_z and the breeding values of the reaction norm parameters $\boldsymbol{\theta}_g$ is the key towards developing
943 a framework that works for any reaction norm, linear in its parameters or not. Let us note \mathcal{A}_θ the
944 vector of breeding values of all the parameters in $\boldsymbol{\theta}$. We will follow the same demonstration as in
945 [de Villemereuil et al. \(2016\)](#), which starts from the point that, by definition, breeding values are all
946 linked through linear relationships (see also [Robertson 1966](#)), since they are all linearly linked to the
947 genotype ([Lynch & Walsh 1998](#)). More precisely, the breeding value \mathcal{A}_z of the phenotypic trait z of
948 an individual linearly depends on a linear combination of its breeding values for the reaction norm
949 parameters \mathcal{A}_θ , so that:

$$\mathcal{A}_z = \mu_A + \mathcal{A}_\theta^T \boldsymbol{\psi} \quad (\text{S11})$$

950 where μ_a is a constant chosen such that $E(\mathcal{A}_z) = 0$, $\boldsymbol{\psi}$ is a vector of slopes that we will shortly describe
951 as the reaction norm gradient.

952 **Derivation of $\boldsymbol{\psi}$** To derive an expression of $\boldsymbol{\psi}$, we can apply the results in Equation S6 to Equa-
 953 tion S11, yielding

$$\boldsymbol{\psi} = \mathbf{G}_\theta^{-1} \text{cov}(\mathcal{A}_\theta, \hat{z}). \quad (\text{S12})$$

954 This assumes that $\text{cov}(\mathcal{A}_\theta, \mathcal{A}_z) = \text{cov}(\mathcal{A}_\theta, \hat{z})$, i.e. that there is no covariance between the environmental
 955 values of the phenotype as predicted by the reaction norm and the breeding values of the parameters.
 956 This results also assumes that \mathbf{G}_θ is invertible. However, such assumption is already necessary to
 957 most statistical algorithms available to infer \mathbf{G}_θ in practice, so that this assumption is not limiting
 958 here. Noting that $\hat{z} = f(\varepsilon, \boldsymbol{\theta})$, we can apply the multivariate version of Stein's lemma (Equation S7):

$$\boldsymbol{\psi} = \mathbf{G}_\theta^{-1} \text{cov}(\mathcal{A}_\theta, \boldsymbol{\theta}_g) \mathbf{E}(\nabla_{\boldsymbol{\theta}} f) = \mathbf{G}_\theta^{-1} \mathbf{G}_\theta \mathbf{E}(\nabla_{\boldsymbol{\theta}} f) = \mathbf{E}(\nabla_{\boldsymbol{\theta}} f), \quad (\text{S13})$$

959 where we have used the fact that the covariance of breeding values of reaction norm parameters with
 960 their breeding values is their additive genetic covariance matrix \mathbf{G}_θ . Again, note that this assumes
 961 that f is partially differentiable with respect to all elements of $\boldsymbol{\theta}_g$. Given that this demonstration was
 962 applied when holding the environment constant, the values in $\boldsymbol{\psi}$ generally depend on the environment
 963 ε , so below and in the main text, we use the notation $\boldsymbol{\psi}_\varepsilon$.

964 **Values of $\boldsymbol{\psi}_\varepsilon$ in specific contexts** When the reaction norm is linear in its parameters, the values
 965 in $\boldsymbol{\psi}_\varepsilon$ are (trivially) the linear coefficients of such relation. For a quadratic reaction norm, where
 966 $\hat{z} = (\bar{\mathcal{A}} + a_g) + (\bar{b} + b_g)\varepsilon + (\bar{c} + c_g)\varepsilon^2$, such linear coefficients are respectively 1, ε and ε^2 for a_g , b_g
 967 and c_g . It results that $\boldsymbol{\psi}_\varepsilon = (1, \varepsilon, \varepsilon^2)^T$ as mentioned in the main text. More generally, if f is a
 968 polynomial of order N , then $\boldsymbol{\psi}_\varepsilon = (1, \varepsilon, \dots, \varepsilon^N)^T$. In the context of a character-state, it can be seen
 969 from Equation S4 that the gradient $\boldsymbol{\psi}_\varepsilon$ in the parameters will be equal to \mathbf{u}_k , i.e. a vector of 1 for the
 970 k th value (corresponding to the environment chosen to be hold constant) and 0 elsewhere.

971 **B3 Additive genetic variance**

972 By definition, the additive genetic variance of the trait conditional on the environment $V_{A|\varepsilon}$ is the
 973 variance of the breeding values defined in Equation S11. We can thus express it from the breeding
 974 values of the reaction norm parameters (right hand side of Equation S11) as

$$V_{A|\varepsilon} = V_{g|\varepsilon}(\mathcal{A}_\theta^T \boldsymbol{\psi}_\varepsilon) = \boldsymbol{\psi}_\varepsilon^T \mathbf{G}_\theta \boldsymbol{\psi}_\varepsilon. \quad (\text{S14})$$

975 This formula holds whether the reaction norm is linear on its parameters or not, and also holds for
 976 the character-state approach (although in this case, this formula merely selects the k th element of the

977 diagonal of \mathbf{G}_z).

978 **C Derivation of the general decomposition of variance**

979 **C1 Distinguishing between V_{Plas} , V_{Gen} and V_{Add}**

980 The phenotype predicted by the reaction norm \hat{z} depends on the environment, and the reaction norm
 981 parameters θ_g specific to the genotype g . The impacts of environment and genotype are intricately
 982 related via the reaction norm shape, but in a given environment, one can still isolate the average
 983 impact of the environment from variation among genotypes by computing the average value of the
 984 reaction norm across genotypes conditional on the environment, i.e. $\mathbf{E}_{g|\varepsilon}(\hat{z})$. The variance of $\mathbf{E}_{g|\varepsilon}(\hat{z})$,
 985 taken across environments, is the component $V_{\text{Plas}} = \mathbf{V}(\mathbf{E}_{g|\varepsilon}(\hat{z}))$ in the main text, i.e. the phenotypic
 986 variance arising from plasticity after averaging across genotypes. The genotypic value \mathcal{G}_z of genotype
 987 g within the environment ε is then given by

$$\mathcal{G}_z = \hat{z} - \mathbf{E}_{g|\varepsilon}(\hat{z}). \quad (\text{S15})$$

988 Note that, although we removed the average effect of the environment, the genotypic value \mathcal{G}_z still
 989 depends on both the genotype g and the environment ε , because genotypes can vary in their response
 990 to the environment. The total genetic variance in the reaction norm is thus $V_{\text{Gen}} = \mathbf{V}(\mathcal{G}_z)$. It is possible
 991 to get to the breeding values of the trait in each environment \mathcal{A}_z following the process described in
 992 [Appendix B](#), i.e. $\mathcal{A}_z = \mu_a + \mathcal{A}_\theta^T \psi_\varepsilon$. The total additive genetic variance in the reaction norm is then

$$V_{\text{Add}} = \mathbf{V}(\mathcal{A}_z) = \mathbf{E}(\mathbf{V}_{g|\varepsilon}(\mathcal{A}_z)) + \mathbf{V}(\mathbf{E}_{g|\varepsilon}(\mathcal{A}_z)) = \mathbf{E}(\psi_\varepsilon^T \mathbf{G}_\theta \psi_\varepsilon), \quad (\text{S16})$$

993 using the law of total variance and noting that $\mathbf{E}_{g|\varepsilon}(\mathcal{A}_z) = 0$ by construction. In [Figure 1](#) in the main
 994 text, the average $\mathbf{E}_{g|\varepsilon}(\hat{z})$ corresponds to the red line in the left panel of [Figure 1](#) in the main
 995 text, while \mathcal{A}_z corresponds to the purple lines in the middle panel.

996 **C2 Distinguishing between V_{Add} , V_{A} and $V_{\text{A} \times \text{E}}$**

997 We can separate the total additive genetic variance of the reaction norm, V_{Add} , into two components:
 998 the marginal additive genetic variance of the trait V_{A} and the additive genetic variance of plasticity
 999 $V_{\text{A} \times \text{E}}$. The first component is given by considering, for a given genotype, its average breeding value

1000 across environment:

$$\bar{\mathcal{A}} = \mathbb{E}_{\varepsilon|g}(\mathcal{A}_z). \quad (\text{S17})$$

1001 This average corresponds to the breeding value that would be predicted for the same genotype present
 1002 in all environments (or moving across them, being measured several times), ignoring the impact of
 1003 the environment. In other words, this average is the predicted breeding value after the impact of
 1004 the environment has been marginalised. Graphically, it depicts the average shift in the y -axis of the
 1005 reaction norm, as can be seen in the middle panel of [Figure 1](#) in the main text. The marginal additive
 1006 genetic variance of the trait is

$$V_A = V(\bar{\mathcal{A}}) = \mathbb{E}(\boldsymbol{\psi}_\varepsilon)^T \mathbf{G}_\theta \mathbb{E}(\boldsymbol{\psi}_\varepsilon) \quad (\text{S18})$$

1007 The remaining additive genetic variation after accounting for the marginal breeding value is linked
 1008 to the impact of genetic variation in plasticity, arising from genotype-by-environment interactions. We
 1009 can define the part of the breeding values strictly linked to that genotype-by-environment interaction
 1010 by mean-centring the breeding values, for each genotype:

$$\mathcal{A}_I = \mathcal{A}_z - \bar{\mathcal{A}}. \quad (\text{S19})$$

1011 The right panel of [Figure 1](#) depicts these interaction breeding values. The additive genetic variance
 1012 linked to genotype-by-environment, and thus to variation in plasticity, is:

$$V_{A \times E} = V(\mathcal{A}_I) = V(\mathcal{A}_z) + V(\bar{\mathcal{A}}) - 2\text{cov}(\mathcal{A}_z, \bar{\mathcal{A}}) = V(\mathcal{A}_z) - V(\bar{\mathcal{A}}) = V_{\text{Add}} - V_A, \quad (\text{S20})$$

1013 noting that, by construction, $\text{cov}(\mathcal{A}_z, \bar{\mathcal{A}}) = \text{cov}(\bar{\mathcal{A}}, \bar{\mathcal{A}}) = V(\bar{\mathcal{A}})$. By substituting V_{Add} and V_A with
 1014 their values in [Equation S16](#) and [Equation S18](#), we obtain

$$V_{A \times E} = \mathbb{E}(\boldsymbol{\psi}_\varepsilon^T \mathbf{G}_\theta \boldsymbol{\psi}_\varepsilon) - \mathbb{E}(\boldsymbol{\psi}_\varepsilon)^T \mathbf{G}_\theta \mathbb{E}(\boldsymbol{\psi}_\varepsilon) = \text{tr}(\boldsymbol{\Psi} \mathbf{G}_\theta) = \sum_{l,k} \Psi_{l,k} \mathbf{G}_{\theta(l,k)}, \quad (\text{S21})$$

1015 where $\boldsymbol{\Psi}$ is the variance-covariance matrix of the reaction norm gradient $\boldsymbol{\psi}_\varepsilon$ across the environment.
 1016 In other words, $V_{A \times E}$ is the sum of the products, for all pairs of parameters, of the (co)variance in
 1017 the reaction norm gradient and the additive genetic (co)variance. The γ - and ι -decomposition directly
 1018 comes from dividing each elements of the sums in [Equation S16](#) and [Equation S21](#) respectively by
 1019 V_{Add} and $V_{A \times E}$, so that the total sums to 1.

1020 C3 Variance decomposition for a polynomial model

1021 In this section, we will assume a polynomial reaction norm:

$$\hat{z} = \sum_{n=0}^N (\bar{\theta}_n + \theta_{n,g}) \varepsilon^n \quad (\text{S22})$$

1022 where $\theta_n = \bar{\theta}_n + \theta_{n,g}$ is the n th order coefficient of the polynomial. In this form, it is easy to remark
 1023 that polynomial reaction norms are linear in their parameters, i.e. there is a linear relationship between
 1024 the θ_n 's and \hat{z} , so that $\mathcal{G}_z = \mathcal{A}_z$. It results that:

$$\mathcal{G}_z = \mathcal{A}_z = \hat{z} - \mathbf{E}_{g|\varepsilon}(\hat{z}) = \sum_{n=0}^N (\bar{\theta}_n + \theta_{n,g}) \varepsilon^n - \sum_{n=0}^N \bar{\theta}_n \varepsilon^n = \sum_{n=0}^N \theta_{n,g} \varepsilon^n. \quad (\text{S23})$$

1025 Taking the derivative of this expression with respect to each of $\theta_{n,g}$ in a given environment ε would
 1026 yield a reaction norm gradient equal to the value of each exponent of ε , i.e. $\boldsymbol{\psi}_\varepsilon = (1, \varepsilon, \dots, \varepsilon^N)^T$. The
 1027 total (additive) genetic variance is thus:

$$V_{\text{Gen}} = V_{\text{Add}} = \mathbf{E}(\boldsymbol{\psi}_\varepsilon^T \mathbf{G}_\theta \boldsymbol{\psi}_\varepsilon) = \sum_n V_n \mathbf{E}(\varepsilon^{2n}) + 2 \sum_{n < m} C_{nm} \mathbf{E}(\varepsilon^{n+m}), \quad (\text{S24})$$

1028 where V_n is the additive genetic variance for $\theta_{n,g}$ and C_{nm} is the additive genetic covariance between
 1029 $\theta_{m,g}$ and $\theta_{n,g}$. For the quadratic case, if ε has been mean-centred and is symmetrical, we have
 1030 $\mathbf{E}(\varepsilon) = \mathbf{E}(\varepsilon^3) = 0$ and the expression reduces to

$$V_{\text{Gen}} = V_{\text{Add}} = V_0 + (V_1 + C_{03}) \mathbf{E}(\varepsilon^2) + V_3 \mathbf{E}(\varepsilon^4). \quad (\text{S25})$$

1031 For a given genotype, its average breeding value across environments is

$$\bar{\mathcal{A}} = \mathbf{E}_{\varepsilon|g}(\mathcal{A}_z) = \mathbf{E}_{\varepsilon|g} \left(\sum_{n=0}^N \theta_{n,g} \varepsilon^n \right) = \sum_{n=0}^N \theta_{n,g} \mathbf{E}(\varepsilon^n) \quad (\text{S26})$$

1032 The marginal (additive) genetic variance of the trait is

$$V_G = V_A = \mathbf{E}(\boldsymbol{\psi}_\varepsilon)^T \mathbf{G}_\theta \mathbf{E}(\boldsymbol{\psi}_\varepsilon) = \sum_n V_n \mathbf{E}(\varepsilon^n)^2 + 2 \sum_{n < m} C_{nm} \mathbf{E}(\varepsilon^n) \mathbf{E}(\varepsilon^m) \quad (\text{S27})$$

1033 For the quadratic case with mean-centred and symmetrical ε , this yields:

$$V_A = V_0 + 2C_{02} \mathbf{E}(\varepsilon^2) + V_2 \mathbf{E}(\varepsilon^2)^2 \quad (\text{S28})$$

1034 Finally, the additive genetic variance in plasticity itself is

$$V_{A \times E} = V_{\text{Add}} - V_A = \sum_n V_n E(\varepsilon^{2n}) + 2 \sum_{n < m} C_{nm} E(\varepsilon^{n+m}) - \sum_n V_n E(\varepsilon^n)^2 + 2 \sum_{n < m} C_{nm} E(\varepsilon^n) E(\varepsilon^m). \quad (\text{S29})$$

1035 By recognising that $V(\varepsilon^n) = E(\varepsilon^{2n}) - E(\varepsilon^n)^2$ and $\text{cov}(\varepsilon^n, \varepsilon^m) = E(\varepsilon^{n+m}) - E(\varepsilon^n)E(\varepsilon^m)$, we can further
1036 simplify this expression as:

$$V_{A \times E} = \sum_n V_n V(\varepsilon^n) + 2 \sum_{lk} C_{nm} \text{cov}(\varepsilon^n, \varepsilon^m). \quad (\text{S30})$$

1037 For the quadratic case, for a mean-centred and symmetrical ε , all the covariances between the different
1038 exponents of ε are 0, yielding

$$V_{A \times E} = V_1 V(\varepsilon) + V_2 V(\varepsilon^2). \quad (\text{S31})$$

1039 **C4 Variance decomposition for the character-state approach**

1040 As mentioned in [Appendix A](#), the character-state can be written using a function f such that in
1041 environment ε_k and for genotype g , we have

$$\hat{z} = f(\boldsymbol{\mu}_g, \varepsilon_k) = \boldsymbol{\mu}_g^T \mathbf{u}_k. \quad (\text{S32})$$

1042 In a given environment ε_k , the unit vector \mathbf{u}_k is equal to 1 at the k th index and 0 elsewhere. The
1043 reaction norm gradient is equal to this unit vector, i.e. $\boldsymbol{\psi}_{\varepsilon_k} = \mathbf{u}_k$. In the first environment, for example,
1044 we have $\boldsymbol{\psi}_{\varepsilon_1} = \mathbf{u}_1 = (1, 0, \dots)^T$. As mentioned in [Appendix A](#), the character-state approach is linear
1045 in its parameters. We can thus compute the genotypic/breeding values in a given environment ε_k as

$$\mathcal{G}_z = \mathcal{A}_z = \hat{z} - E_{g|\varepsilon}(\hat{z}) = \boldsymbol{\mu}_g^T \mathbf{u}_k - \boldsymbol{\mu}^T \mathbf{u}_k = \mu_{g,k} - \mu_j, \quad (\text{S33})$$

1046 where $\mu_{g,k}$ and μ_j are the k th values of the vectors $\boldsymbol{\mu}_g$ and $\boldsymbol{\mu}$. The total (additive) genetic variance is
1047 the variance of the breeding values across environments:

$$V_{\text{Gen}} = V_{\text{Add}} = V(\mathcal{A}_z) = V(\mu_{g,k}). \quad (\text{S34})$$

1048 Since the variance-covariance matrix of $\boldsymbol{\mu}_g$ is the \mathbf{G}_z matrix, the variance of all elements $\mu_{g,k}$ taken
1049 together is the average of the diagonal elements of \mathbf{G}_z , which we will note V_k . Assuming that all
1050 environments are equiprobable for the sake of simplicity (releasing this assumption merely requires to

1051 use weighted average), we have

$$V_{\text{Add}} = \frac{1}{K} \sum_{k=1}^K V_k. \quad (\text{S35})$$

1052 In other words, V_{Add} is the average of the diagonal elements of the \mathbf{G}_z matrix.

1053 The marginal (additive) genetic variance of the trait depends on the average of the breeding values
1054 across environment for a given genotype:

$$\bar{A} = \frac{1}{K} \sum_k \mathcal{A}_{z,k}, \quad (\text{S36})$$

1055 where $\mathcal{A}_{z,k}$ is the breeding value evaluated at the k th environment for a given genotype, still assuming
1056 equiprobable environments. It results that the marginal (additive) genetic variance of the trait is

$$V_G = V_A = \frac{1}{K^2} \left(\sum_k V_k + 2 \sum_{k<l} C_{kl} \right), \quad (\text{S37})$$

1057 where C_{kl} is the genetic covariance between the environment k and l . In other words, V_A is the average
1058 of all the elements of the \mathbf{G}_z matrix.

1059 Finally, the (additive) genetic variance of plasticity can be computed as the difference between
1060 V_{Add} and V_A :

$$V_{G \times E} = V_{A \times E} = V_{\text{Add}} - V_A = \frac{1}{K^2} \left((K-1) \sum_k V_k - 2 \sum_{k<l} C_{kl} \right) \quad (\text{S38})$$

1061 A few particular cases are important to note here. The first case is when all environments harbour
1062 the same additive genetic variance, say V , and are all perfectly correlated with one another. This is
1063 a situation generally describe as a total absence of genetic variation in plasticity. In our framework,
1064 this situation would indeed result in $V_{\text{Add}} = V_A = V$ and, indeed, no genetic variation in plasticity
1065 with $V_{A \times E} = 0$. Note that uneven additive genetic variances across environments, even if genetic
1066 correlation are kept perfect across environments, would result in slightly positive genetic variance in
1067 plasticity with $V_{A \times E} > 0$. This is because, in such context, the trait can still evolve faster in some
1068 environments compared to other, hence plasticity can evolve. The second extreme case, is when the
1069 marginal additive genetic variance of the trait is null, i.e. $V_A = 0$, while all the additive genetic
1070 variance in reaction norm is composed of the additive genetic variance in plasticity, i.e. $V_{\text{Add}} = V_{A \times E}$.
1071 This happens when the sum of covariances (the total of which must be negative) exactly compensates
1072 the sum of diagonal variances in the \mathbf{G}_z , meaning that strong negative genetic correlation must exist
1073 between environments. In this case, its is impossible for directional selection to act on average value of
1074 the trait across all environments, but the evolvability of plasticity is maximised. A third, interesting
1075 case is when there is absolutely no genetic correlation between environments, i.e. the off-diagonal

1076 elements of \mathbf{G}_z are all equal to 0. In such case, it is important to note that, because evolution can
 1077 freely operate across environments, then both $V_A = \frac{1}{K^2} \sum_k V_k$ and $V_{A \times E} = \frac{K-1}{K^2} \sum_k V_k$ are non-zero.

1078 **D Derivation of π - and φ -partition of V_{Plas}**

1079 **D1 The π -decomposition**

1080 We have seen in [Appendix C](#) how to compute the variance arising from the average shape of reaction
 1081 norm V_{Plas} . In order to go further, we now separate this into a component linked to the average slope
 1082 of the reaction norm and another linked to the average curvature. For this, we need one or two of
 1083 the following assumptions to hold true: (i) the environment ε follows a normal distribution; or (ii)
 1084 the function f is quadratic. In such context, we can isolate the contribution of the slope, V_{Sl} , from
 1085 the contribution of the curvature, V_{Cv} to V_{Plas} , based on the best quadratic approximation of $E_{g|\varepsilon}(\hat{z})$
 1086 (akin to the reasoning in Lande & Arnold 1983, for estimates of selection gradients), as:

$$V_{\text{Sl}} = E \left(\frac{dE_{g|\varepsilon}}{d\varepsilon}(\hat{z}) \right)^2 V(\varepsilon), \quad V_{\text{Cv}} = \frac{1}{4} E \left(\frac{d^2 E_{g|\varepsilon}}{d\varepsilon^2}(\hat{z}) \right)^2 V(\varepsilon^2). \quad (\text{S39})$$

1087 As an illustration of why the assumptions above are needed, if ε follows a uniform distribution between
 1088 -2 and 2; and the average shape of plasticity is the following cubic function, $f(\varepsilon) = 2\varepsilon - 0.5\varepsilon^2 - \varepsilon^3$,
 1089 then the average slope is -2, while the slope from the best quadratic approximation of $E_{g|\varepsilon}(\hat{z})$ is -0.4.
 1090 In such cases, the decomposition in [Equation S39](#) is not valid anymore, due to (i) the impossibility
 1091 to apply Stein's lemma to a non-normal distribution and (ii) strong covariation between the slope
 1092 and curvature. This means that whenever the environment is non-normal and the reaction norm is
 1093 non-quadratic, the π -decomposition can bear little meaning (in the cubic example above, V_{Sl} would
 1094 be 5.4, while $V_{\text{Plas}} = 2.0$, so that π_{Sl} would be largely above 1). A truly quadratic reaction norm is
 1095 the only case where $\pi_{\text{Sl}} + \pi_{\text{Cv}} = 1$.

1096 **D2 The φ -decomposition**

1097 In such cases where the environment is non-normal and the reaction norm is non-quadratic, it is always
 1098 possible to approximate the true shape of the reaction norm using a polynomial function:

$$\hat{z} = \sum_{n=0}^N (\bar{\theta}_n + \theta_{n,g}) \varepsilon^n \quad (\text{S40})$$

1099 In the context of decomposing V_{Plas} , such polynomial approximation provides a possibility to isolate
 1100 the (co-)contribution of the (pairs of) coefficients in $E_{g|\varepsilon}(\hat{z}) = \sum_{n=0}^N \bar{\theta}_n \varepsilon^n$:

$$V_{\text{Plas}} = V(E_{g|\varepsilon}(\hat{z})) = \sum_n \bar{\theta}_n^2 V(\varepsilon^n) + 2 \sum_{n < m} \bar{\theta}_n \bar{\theta}_m \text{cov}(\varepsilon^n, \varepsilon^m) \quad (\text{S41})$$

1101 From this, we suggest the alternative φ -decomposition of V_{Plas} , with $\varphi_n = \frac{\bar{\theta}_n^2 V(\varepsilon^n)}{V_{\text{Plas}}}$ and $\varphi_{nm} =$
 1102 $\frac{2\bar{\theta}_n \bar{\theta}_m \text{cov}(\varepsilon^n, \varepsilon^m)}{V_{\text{Plas}}}$. It is important to note that this decomposition is based on the *coefficients* of the
 1103 polynomial function and, thus, it is unfortunately impossible to simply interpret the φ_n in terms of
 1104 slope (for φ_1), curvature (for φ_2), and so on. The only exception is when the reaction norm shape is
 1105 quadratic, in which case $\pi_{\text{SI}} = \varphi_1$ and $\pi_{\text{CV}} = \varphi_2$.

1106 E Correcting for uncertainty in the estimation of fixed 1107 effects

1108 **Character-state approach** It is easier to start with the character-state approach based on the
 1109 ANOVA model. We want to compute V_{Plas} as the variance of the group-level effects μ :

$$V_{\text{Plas}} = V(\mu) \quad (\text{S42})$$

1110 However, we do not have access to the real-world values for μ , but only to the estimated $\hat{\mu}$ from the
 1111 model. Such estimates, if unbiased, have an expected value of μ_k in environment k and a standard-
 1112 error (i.e. the estimation of the sampling standard deviation) s_k . In other words, we can state that
 1113 $\hat{\mu}_k$ is equal to μ_k up to an additive error:

$$\hat{\mu}_k = \mu_k + \tilde{\mu}_k \quad (\text{S43})$$

1114 where $\tilde{\mu}$ is of mean 0 and variance s_k^2 . Considering each virtual repeat r of the experiment, we can
 1115 apply the law of total variance:

$$V(\hat{\mu}) = V_\varepsilon(E_{r|\varepsilon}(\hat{\mu})) + E_\varepsilon(V_{r|\varepsilon}(\hat{\mu})) = V_\varepsilon(\mu) + E_\varepsilon(s^2). \quad (\text{S44})$$

1116 We thus have:

$$V_{\text{Plas}} = V_\varepsilon(\mu) = V_\varepsilon(\hat{\mu}) - E_\varepsilon(s^2) \quad (\text{S45})$$

1117 This result is equivalent to e.g. the classical computation of the “sire variance” in sire models in
 1118 quantitative genetics (Lynch & Walsh 1998), although the latter is generally expressed using sums-of-
 1119 squares.

1120 **Curve-parameter approach** There is unfortunately no simple solution to the problem of accounting
 1121 for the uncertainty of fixed effects in the general context of non-linear modelling. However, for the
 1122 particular case where the model can be framed as a linear model, as is the case for the polynomial
 1123 function, then $\hat{z} = \mathbf{X}\boldsymbol{\theta}$, where \mathbf{X} is the design matrix containing the values for the environment.
 1124 Noting $\boldsymbol{\Sigma}_X$ the variance-covariance matrix of \mathbf{X} , we can define V_{Plas} as:

$$V_{\text{Plas}} = \boldsymbol{\theta}^T \boldsymbol{\Sigma}_X \boldsymbol{\theta}. \quad (\text{S46})$$

1125 Again, the problem is that $\boldsymbol{\theta}$ is unknown, we only have access to the estimated values of the parameters,
 1126 $\hat{\boldsymbol{\theta}}$, that are inferred with an error provided by the variance-covariance matrix of standard errors, \mathbf{S}_θ .
 1127 We can write again:

$$\hat{\boldsymbol{\theta}} = \bar{\boldsymbol{\theta}} + \tilde{\boldsymbol{\theta}}, \quad (\text{S47})$$

1128 Noting that the error is independent from the true value, we have:

$$\hat{\boldsymbol{\theta}}^T \boldsymbol{\Sigma}_X \hat{\boldsymbol{\theta}} = \boldsymbol{\theta}^T \boldsymbol{\Sigma}_X \boldsymbol{\theta} + \tilde{\boldsymbol{\theta}}^T \boldsymbol{\Sigma}_X \tilde{\boldsymbol{\theta}} \quad (\text{S48})$$

1129 To express $\tilde{\boldsymbol{\theta}}^T \boldsymbol{\Sigma}_X \tilde{\boldsymbol{\theta}}$, it is important to note that $S_{\theta,ij} = E(\tilde{\theta}_i \tilde{\theta}_j)$, since $E(\tilde{\boldsymbol{\theta}}) = \mathbf{0}$. Then, we can note
 1130 that, the error being unknown, we actually want to compute $E_r(\tilde{\boldsymbol{\theta}}^T \boldsymbol{\Sigma}_X \tilde{\boldsymbol{\theta}})$ taken across virtual repeats
 1131 r of the experiment:

$$E_r(\tilde{\boldsymbol{\theta}}^T \boldsymbol{\Sigma}_X \tilde{\boldsymbol{\theta}}) = E_r\left(\sum_{ij} \tilde{\theta}_i \tilde{\theta}_j \Sigma_{X,i,j}\right) = \sum_{ij} E_r(\tilde{\theta}_i \tilde{\theta}_j) \Sigma_{X,i,j} = \sum_{ij} S_{\theta,ij} \Sigma_{X,i,j} = \text{Tr}(\mathbf{S}_\theta \boldsymbol{\Sigma}_X) \quad (\text{S49})$$

1132 This is similar to the result of Brown & Rutemiller (1977). Finally, we have:

$$V_{\text{Plas}} = \hat{\boldsymbol{\theta}}^T \boldsymbol{\Sigma}_X \hat{\boldsymbol{\theta}} - \text{Tr}(\mathbf{S}_\theta \boldsymbol{\Sigma}_X). \quad (\text{S50})$$

1133 **F Full results for the section “Perfect modelling of**
 1134 **quadratic curves”**

1135 This section provides the full results corresponding to the section “Perfect modelling of quadratic
 1136 curves” in the main text. The results of all investigated values for the number of environments (10
 1137 or 4) and number of genotypes (20 or 5 for the discrete case, 200 or 50 for the continuous case) are
 1138 provided for the discrete and continuous cases.

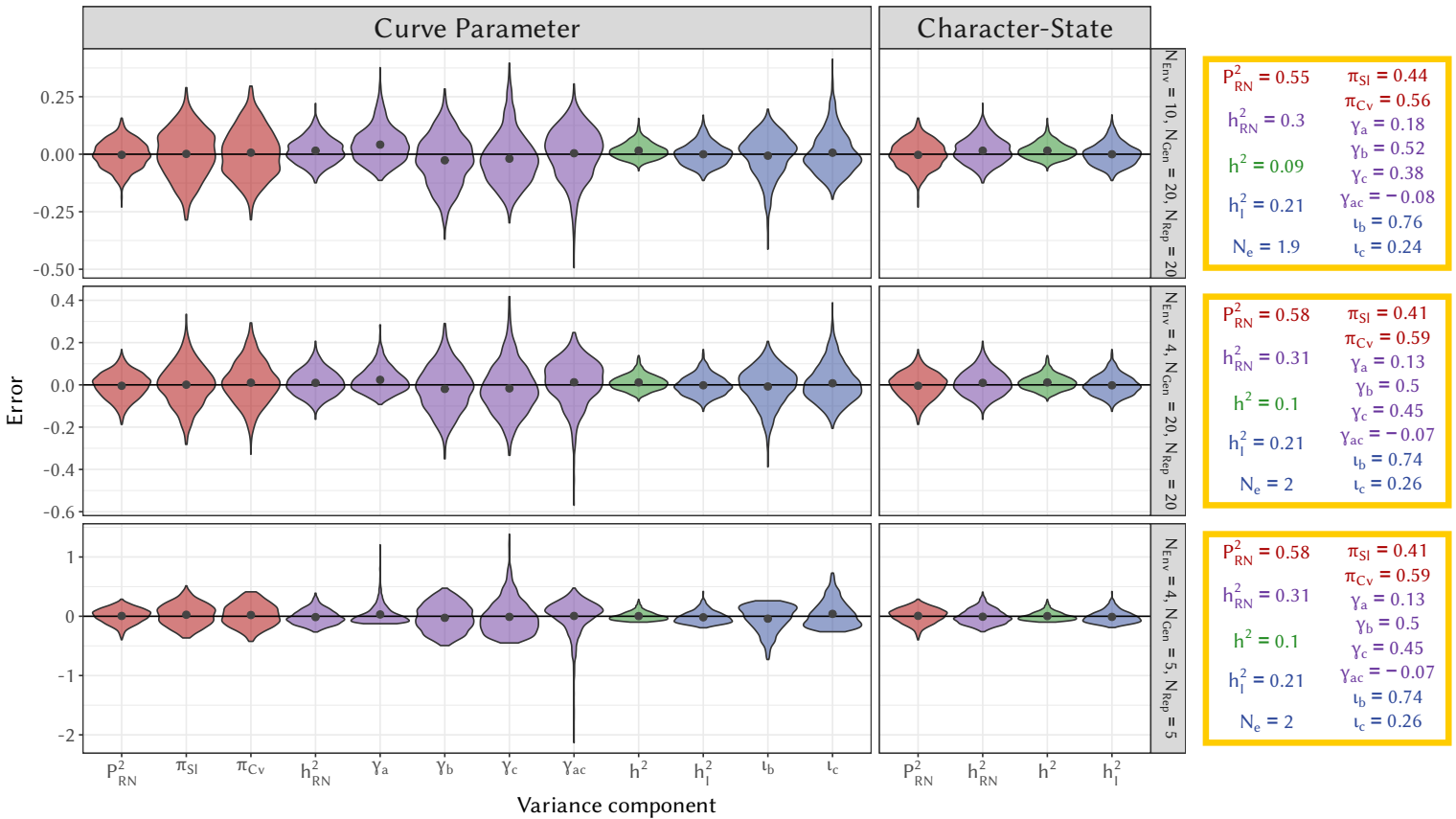


Figure S1: Distribution of the error (difference between the inferred and true value) for each the inferred variance components for three discrete scenarios: N_{env} : number of environments, N_{Gen} : number of different genotypes, N_{Rep} : number of replicates per genotype. Estimates are for \hat{P}_{RN}^2 (proportion of variance generated by plasticity after averaging across genotypes), \hat{h}_{RN}^2 (total heritability of the reaction norm), \hat{h}^2 (heritability based on average breeding values) and \hat{h}_I^2 (heritability of plasticity) for both the curve-parameter and character-state approaches. For the curve-parameter, the π -decomposition of \hat{P}_{RN}^2 into π_{SI} (contribution of the slope) and π_{Cv} (contribution of the curvature); the γ -decomposition of \hat{h}_{RN}^2 into γ_a (genetic contribution of the intercept), γ_b (genetic contribution of the slope), γ_c (genetic contribution of the curvature) and γ_{ac} (genetic contribution of the covariance between the intercept and the curvature) and the l -decomposition of \hat{h}_I^2 into l_b (slope) and l_c (curvature) are also shown. The grey dots correspond to the average over the 1000 simulations. The effective number of dimensions n_e from the character-state is not shown, due to an important bias impacting the comparison with the other parameters.

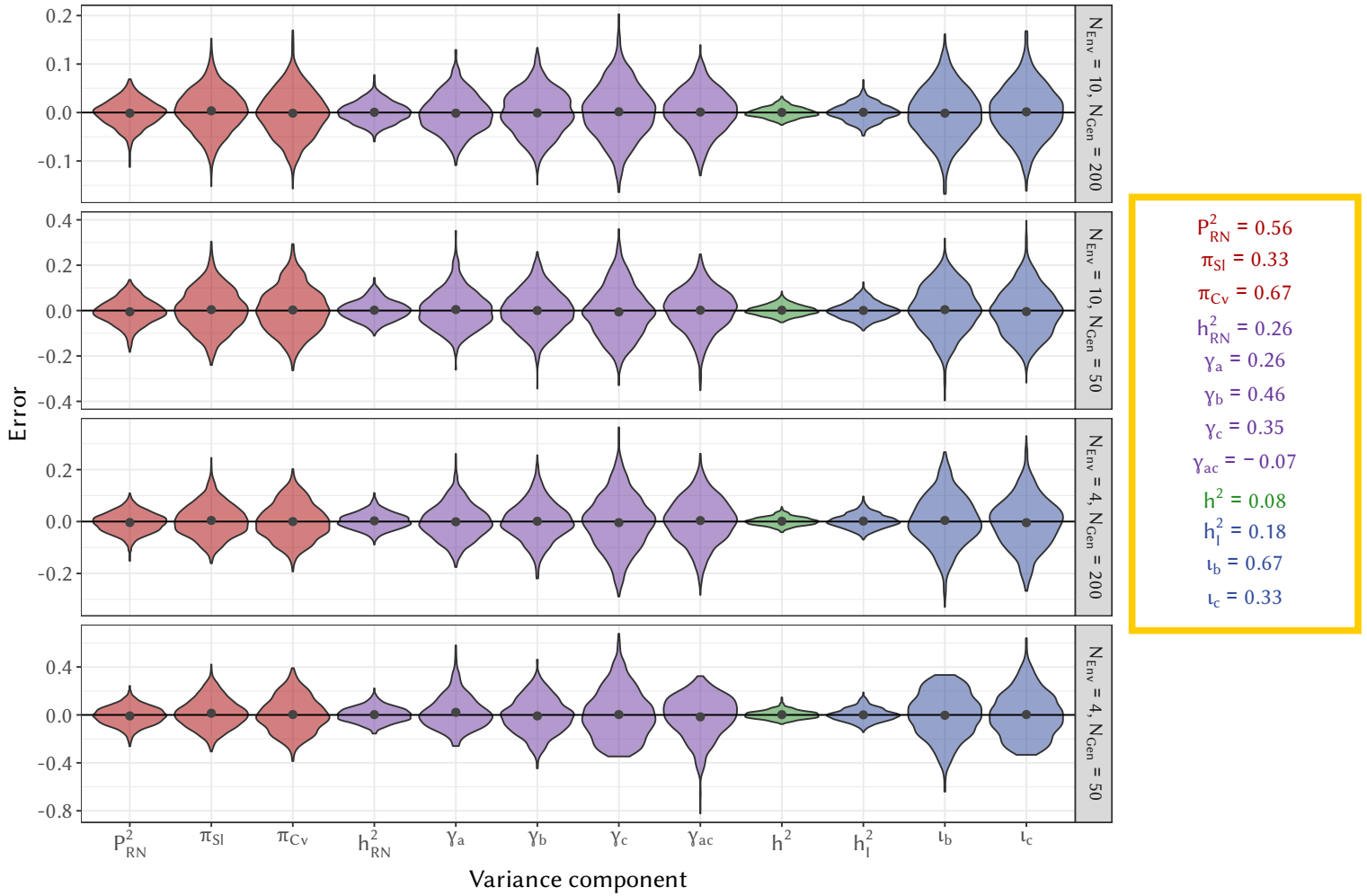


Figure S2: Distribution of the error (difference between the inferred and true value) for each the inferred variance components for four continuous scenarios: N_{env} : number of environment tested per genotype, N_{Gen} : number of different genotypes. The character-state approach was impossible for the continuous environment scenario. Estimates are for \hat{P}^2_{RN} (proportion of variance generated by plasticity after averaging across genotypes), \hat{h}^2_{RN} (total heritability of the reaction norm), \hat{h}^2 (heritability based on average breeding values) and \hat{h}^2_l (heritability of plasticity) for both the curve-parameter and character-state approaches. For the curve-parameter, the π -decomposition of \hat{P}^2_{RN} into π_{SI} (contribution of the slope) and π_{Cv} (contribution of the curvature); the γ -decomposition of \hat{h}^2_{RN} into γ_a (genetic contribution of the intercept), γ_b (genetic contribution of the slope), γ_c (genetic contribution of the curvature) and γ_{ac} (genetic contribution of the covariance between the intercept and the curvature) and the l -decomposition of \hat{h}^2_l into l_b (slope) and l_c (curvature) are also shown. The grey dots correspond to the average over the 1000 simulations. The effective number of dimensions n_e from the character-state is not shown, due to an important bias impacting the comparison with the other parameters.

1139 G Comparison with the approach from Murren *et al.* (2014)

1140 Murren *et al.* (2014) studied variation of the reaction norm shapes across different datasets, using
 1141 their own metrics. We argue in the main text that our variance decomposition is more appropriate
 1142 than the ones suggested by Murren *et al.* (2014), and we develop here why.

1143 The first step in the approach of Murren *et al.* (2014) is to choose a reference reaction norm in
 1144 each of the studies and compute contrasts (i.e. difference with) to that particular reaction norm. The

1145 contrasts are then analysed, rather than the reaction norms themselves. For the sake of simplicity,
 1146 and because this does not (or marginally) impact our comments on this approach, we will overlook
 1147 that step and consider reaction norms directly.

1148 For each genotype k and from its given reaction norm (or contrast) $\mathbf{z}_k = \{z_{k,1}, \dots, z_{k,n}\}$, Murren et al.
 1149 (2014) compute four statistics (we removed the absolute values for the sake of simplicity here):

1150 1. The offset, O_M , measures the “location” of the reaction norm, i.e. its mean. Comparison of
 1151 the offsets allows detecting whether reaction norms are “shifted” toward higher or lower values.
 1152 It is computed, for each genotype k , as the absolute value of the average of the norm across
 1153 environments:

$$O_{M,k} = \frac{\sum_i^n |z_{k,i}|}{n}. \quad (\text{S51})$$

1154 2. The slope, S_M , measures the linear trend of the reaction norms. Formally, it is the absolute sum
 1155 of the differences between two consecutive environments, divided by the number of intervals
 1156 ($n - 1$):

$$S_{M,k} = \frac{\sum_i^{n-1} |z_{k,i+1} - z_{k,i}|}{n - 1}. \quad (\text{S52})$$

1157 3. The curvature, C_M , is computed as the absolute value of the average change in phenotype
 1158 between two consecutive pairs of environments:

$$C_{M,k} = \frac{\sum_i^{n-2} |(z_{k,i+2} - z_{k,i+1}) - (z_{k,i+1} - z_{k,i})|}{n - 2}. \quad (\text{S53})$$

1159 4. The wiggle, W_M , is, according to the authors the “the variability in shape not described by any
 1160 of the previous three measures”:

$$W_{M,k} = \frac{\sum_i^{n-2} |(z_{k,i+2} - z_{k,i+1}) - (z_{k,i+1} - z_{k,i})|}{n - 2} - C_{M,k}. \quad (\text{S54})$$

1161 Given the lower interest in this latter statistics, we will not comment on it any further. Most of
 1162 the comments on the other statistics also apply to this one.

1163 One strong assumption underlying the calculations above is that environmental values $\varepsilon = \{\varepsilon_1, \dots, \varepsilon_n\}$
 1164 on which the reaction norms were evaluated are evenly spaced, e.g. that the differences $\varepsilon_{i+1} - \varepsilon_i$ are
 1165 equal for all possible values of i . The assumption is actually that the space between two measures
 1166 is equal to 1 (which, admittedly, is only a matter of rescaling when evenly-spaced values are already
 1167 assumed). If this is the case, then there is indeed no loss in generality in using the number of
 1168 components (n , $n - 1$ and $n - 2$) rather than actual values of x in the denominator. Although it is

1169 common for studies on reaction norms to use evenly-spaced environmental values, it is an unnecessary
1170 assumption that shall not be satisfied by all studies.

1171 Second, developing the sums in S_M and C_M above show that the intermediate values cancel each other
1172 out, leaving only the values at each extreme of the environmental range in the estimate:

$$\begin{aligned} S_{M,k} &= \frac{z_{k,n} - z_{k,1}}{n - 1}, \\ C_{M,k} &= \frac{(z_{k,n} - z_{k,n-1}) - (z_{k,2} - z_{k,1})}{n - 2}. \end{aligned} \tag{S55}$$

1173 The issue here is double: *(i)* the estimation is highly sensitive to the random noise coming from a
1174 small number of values (two or three/four); and *(ii)* the intermediate values in the reaction norm are
1175 simply thrown out and not used for a more robust estimation. In other words, it would have been
1176 exactly the same to not measure the reaction norm at these intermediate values, since they are not
1177 accounted for in the calculation.

1178 A final issue is that the approach uses the measured values of the reaction norms without accounting
1179 for the uncertainty in their estimation (i.e. standard-deviation and sample size for each genotype and
1180 environmental value) which poses the well-known issue of non-propagation of the error when doing
1181 “statistics on statistics”.

1182 Although we also provide estimators of the impact of several aspects of reaction norms on the
1183 phenotypic variation, our approach differs from the one from Murren *et al.* (2014) by many aspects.
1184 First, our variance decomposition makes the explicit distinction between the average shape of the
1185 reaction norm and the genetic variance surrounding it. As such, to O_M , S_M and C_M corresponds not
1186 only the π -, but also the γ - and ι -decomposition. We clearly delimit the domain of validity of each of
1187 these decomposition. We also account for possible correlation between those components. Second, we
1188 use the whole of the statistical inference to define our variance decomposition estimates. Third, we
1189 explicitly account for the uncertain estimation of reaction norms.